第91卷 第11期
2017年11月 2387～2408
地 质 学 报 ACTA GEOLOGICA SINICA
Vol. 91 No. 11 2017
Nov. 2387～2408

扬子板块北缘花山群沉积时代及其对Rodinia超大陆裂解的制约

田辉[1)]，李怀坤[1)]，周红英[1)]，张健[1)]，张阔[1)]，耿建珍[1)]，相振群[1)]，瞿乐生[2)]

1）中国地质调查局天津地质调查中心，天津，300170；2）湖北省区域地质矿产调查所，武汉，430034

内容提要：出露于扬子板块北缘大洪山地区的花山群自下而上由一套以砾岩为主的粗碎屑沉积和一套以砂质板岩为主的细碎屑沉积组成，伴随有拉斑玄武质岩浆活动。花山群整体变质程度不高，形成构造环境复杂，对其构造属性及其与区内所谓的花山"蛇绿混杂岩"的时空关系一直存有争议，它们对新元古代Rodinia超大陆在扬子板块北缘的汇聚-裂解响应具有重要的制约意义。笔者在花山群六房咀组下部细砂岩中采集玄武质熔结凝灰岩夹层样品1件，碎屑岩样品2件，在上覆地层南华系莲沱组采集碎屑岩样品1件；对玄武质熔结凝灰岩进行了SHRIMP锆石U-Pb同位素测年，对碎屑岩样品进行了LA-MC-ICPMS锆石U-Pb同位素测年。获得玄武质熔结凝灰岩锆石U-Pb年龄814.7±7.3 Ma；花山群的碎屑锆石U-Pb年龄谱存在三个明显的峰值：～900 Ma、～2050Ma和～2650 Ma，最显著峰值为～2650 Ma，上覆莲沱组碎屑岩年龄谱的三个峰值为：～900 Ma、～2050 Ma和～2500 Ma，最显著峰值为～2050 Ma，三件碎屑岩样品均与扬子板块的碎屑锆石U-Pb年龄统计峰值一致。花山群的碎屑源区可能包括下伏中元古代打鼓石群、太古宙鱼洞子杂岩以及崆岭杂岩。结合前人年代学研究资料和区域构造成果分析，花山群沉积时代应为820～815 Ma，形成于伸展构造背景，与花山"蛇绿混杂岩"不是同期同构造背景的产物；花山"蛇绿混杂岩"与花山群沉积建造依次反映了扬子板块北缘由挤压构造背景向伸展构造背景的转换过程。花山群中的碎屑沉积物与基性火山岩、火山碎屑岩属于裂解背景下形成的同时代沉积-火山建造；结合前人在扬子板块周缘发现的大量约820 Ma酸性—基性岩浆活动记录以及同时代（820～800 Ma）的沉积地层，推测花山群形成于Rodinia超大陆裂解背景之下，与超级地幔柱活动有关。

关键词：扬子板块；大洪山；花山群；Rodinia超大陆

1300～900 Ma之间，地球上几乎所有的古大陆都卷入到Rodinia超大陆的汇聚过程之中（Li Zhengxiang, 1999; Li Zhengxiang et al., 1999, 2008; Lu Songnian et al., 2001, 2012; Rogers and Santosh, 2002; Zhao Guochun et al., 2002; Hoffman, 2007; Evans and Mitchell, 2011; Meert, 2012），860～840 Ma由于超级地幔柱作用，Rodinia超大陆开始了多期次的裂解，造就了825～740 Ma广泛分布的大陆裂谷记录（Larson, 1991; Santosh et al., 2009）。作为Rodinia超大陆的重要组成部分，华南板块主要由扬子板块和华夏板块构成，其对Rodinia超大陆新元古代的汇聚和裂解事件的响应成为近年来的研究热点。新元古代时期扬子板块周缘发育大规模的岩浆作用，成岩时代集中在850～630 Ma之间，包括酸性岩浆侵入、镁铁质—超镁铁质岩浆侵入，并广泛发育同时期火山一沉积建造（Li Zhengxiang et al., 1995; Li Zhengxiang, 1999; Li Xianhua et al., 2002, Wang Xiaolei et al., 2014a; Li Zuochen et al., 2015）。

扬子板块东南缘与华夏板块相接，西缘与青藏高原相连，北部则以秦岭-大别-苏鲁造山带与华北板块相隔。扬子板块周缘在新元古代经历了大洋板块的俯冲和陆缘裂解作用（Li Xianhua et al., 1994; Ling Wenli et al., 2002; Li Zhengxiang et al., 2003），但其俯冲-伸展转换机制和时限仍存在诸多争议：其中扬子板块东南缘与华夏板块的拼合机制较为明确，以四堡群的变质及江南褶皱带的形成为标志，时间在830 Ma左右，并在约815 Ma之后发生了陆内裂解（Wang Jian et al., 2003, Zhang Qirui et al., 2008; Zhao Junhong et al., 2011）；但其北缘

注：本文为中国地质调查局项目（编号DD20160343-06）和湖北省国土资源厅项目"神农架群岩石地层序列和年代格架研究"联合资助成果。

收稿日期：2017-03-27；改回日期：2017-06-15；责任编辑：周健。

作者简介：田辉，男，1985年生。硕士，工程师，地层学专业，主要从事前寒武纪地质调查与研究。Email：309702629@qq.com。

和西缘的构造机制则不甚明确(Yan Quanren et al.,2003),持地幔柱和裂谷模式观点的学者认为北缘和西缘与东南缘具有一致的动力学机制(Li Xianhua et al.,1999,2003;Zheng Yongfei et al.,2007),持岛弧模式观点的学者则认为950～735 Ma扬子板块西缘和北缘仍属于活动大陆边缘(Zhou Meifu and Michael,2002,Zhou Meifu et al.,2006;Zhao Junhong and Zhou Meifu,2007a,2007b,2008,2009a,2009b)。而且对于新元古代中期(825～740 Ma)扬子板块周缘岩浆活动的成因亦有多种解释:地幔柱主导的Rodinia超大陆裂解(Li Xianhua et al.,1999,2002,2003,2008a,2008b;Zhu Weiguang et al.,2006;Lin Guangchun et al.,2007;Wang Lijuan et al.,2011)、活动大陆边缘弧-陆碰撞垮塌熔融(Wang Xiaolei et al.,1982,2004,2006,2014b;Zhou Jincheng et al.,2004;Zhou Meifu et al.,2002;Wang Wei et al.,2012)以及岛弧成因(Zhou Meifu et al.,2006)等。

扬子板块北缘的大洪山地区作为研究古板块拼合—裂解构造机制转换的热点区域,一直受到广泛关注(Zhang Zhongying et al.,1989;Dong Yunpeng et al.,1998,1999,2003;Shi Yuruo et al.,2007;Deng Qi et al.,2013)。大洪山地区北部以襄樊-广济断裂带与秦岭造山带(Wang Tao et al.,2005;Xu Zhiqin et al.,2015)南缘相连,区内存在的"蛇绿混杂岩带"(Dong Yunpeng et al.,1998)及沉积岩组合可能为南秦岭与扬子板块之间存在古洋盆提供重要证据,并进一步提供扬子北缘挤压-伸展机制转换的年代学约束。

围绕大洪山构造带是否为板块结合带及其拼合时代的问题,已有一系列研究成果(Dong Yunpeng et al.,1998,1999,2003;Hu Zhengxiang et al.,2015),作为区内重要的沉积单元,"花山群"成为解决"结合带"构造时限的关键。

"花山群"是由北京大学地质系1959年在1∶20万宜城幅区测报告中首先提出,创立地点为湖北省京山县,原指一套山间河流相粗碎屑和一套浅海相泥质碎屑岩组合,后来1∶20万随县幅❶和宜城幅❷(1982)扩大了其范围,将太阳寺背斜以东的包括酸性—基性火山岩和沉积岩归入其中,可称之为广义的"花山群"。后来几经调整和解体(湖北省地质矿产局,1990;Dong Yunpeng et al.,1998),广义的"花山群"解体为以下三个地质单元:① 襄樊-广济断裂范围内的构造侵位的花山蛇绿混杂岩带;② 大洪山以西的"随县群"构造块体;③ 单一的碎屑沉积建造,该碎屑沉积建造称为狭义的"花山群",时代置于新元古代。

前人在狭义的"花山群"中获得玄武岩的年龄约为820 Ma(Deng Qi et al.,2013),但测年锆石来自基性岩石,其锆石成因仍可能引起质疑,例如在基性岩浆中硅不饱和条件下锆石如何结晶等问题。当然,已有很多在基性岩甚至超基性岩中选取锆石并进行U-Pb定年取得成功的例证(例如liermann et al.,2002;Garnier et al.,2005;Li Huaikun et al.,2013等)。总之,狭义的"花山群"年龄制约尚显不够充分,仍有待进一步研究限定。

本文作者对大洪山地区狭义的"花山群"(后文中简称"花山群")上部六房咀组的玄武质熔结凝灰岩、六房咀组碎屑岩,以及上覆的南华系莲沱组碎屑岩进行了系统的锆石U-Pb年代学研究,以期对花山群进行进一步年龄标定。

1 地质背景

大洪山地区位于湖北省京山县、钟祥县交界处,构造位置属南襄盆地以东、桐柏山南侧,横跨南秦岭与扬子板块(区内以三里岗-三阳断裂带为界),呈北西—南东向展布,主体分布在襄樊-广济(三里岗-三阳)断裂带南西侧的扬子板块(Dong Yunpeng et al.,2003)(图1)。

大洪山地区主要出露的前寒武纪地层包括浅变质的中元古代打鼓石群、新元古代"花山群"和花山蛇绿混杂岩以及几乎未变质的南华纪—震旦纪地层。显生宙地层主要分布在区内主断裂的北东和南西两侧,包绕前寒武纪地质体。其中花山蛇绿混杂岩(图1中浅绿色部分)呈带状展布于三里岗—三阳一线,本身为主断裂所夹持,为一套基性岩为主的岩浆杂岩,包括变玄武岩、辉绿岩、辉长岩、凝灰质角砾岩、石英角斑岩,夹石英绢云千枚岩、泥质板岩等,由于缺乏火山岩的年代学证据,前人将其统称为花山蛇绿混杂岩(Dong Yunpeng et al.,1999),将其与勉略蛇绿岩(Xie Jifeng and Zhang Benren,2000;Li Sanzhong et al.,2002)相对比,认为可能与襄樊-广济断裂印支期以来经历的逆冲推覆和走滑伸展作用的反复叠加有关。之后,根据花山蛇绿混杂岩带中岩浆岩年代学证据,推断其属于晋宁期结合带(Shi Yuruo et al.,2007;Hu Zhengxiang et al.,2015)。

花山群出露于大洪山地区中部,花山蛇绿混杂

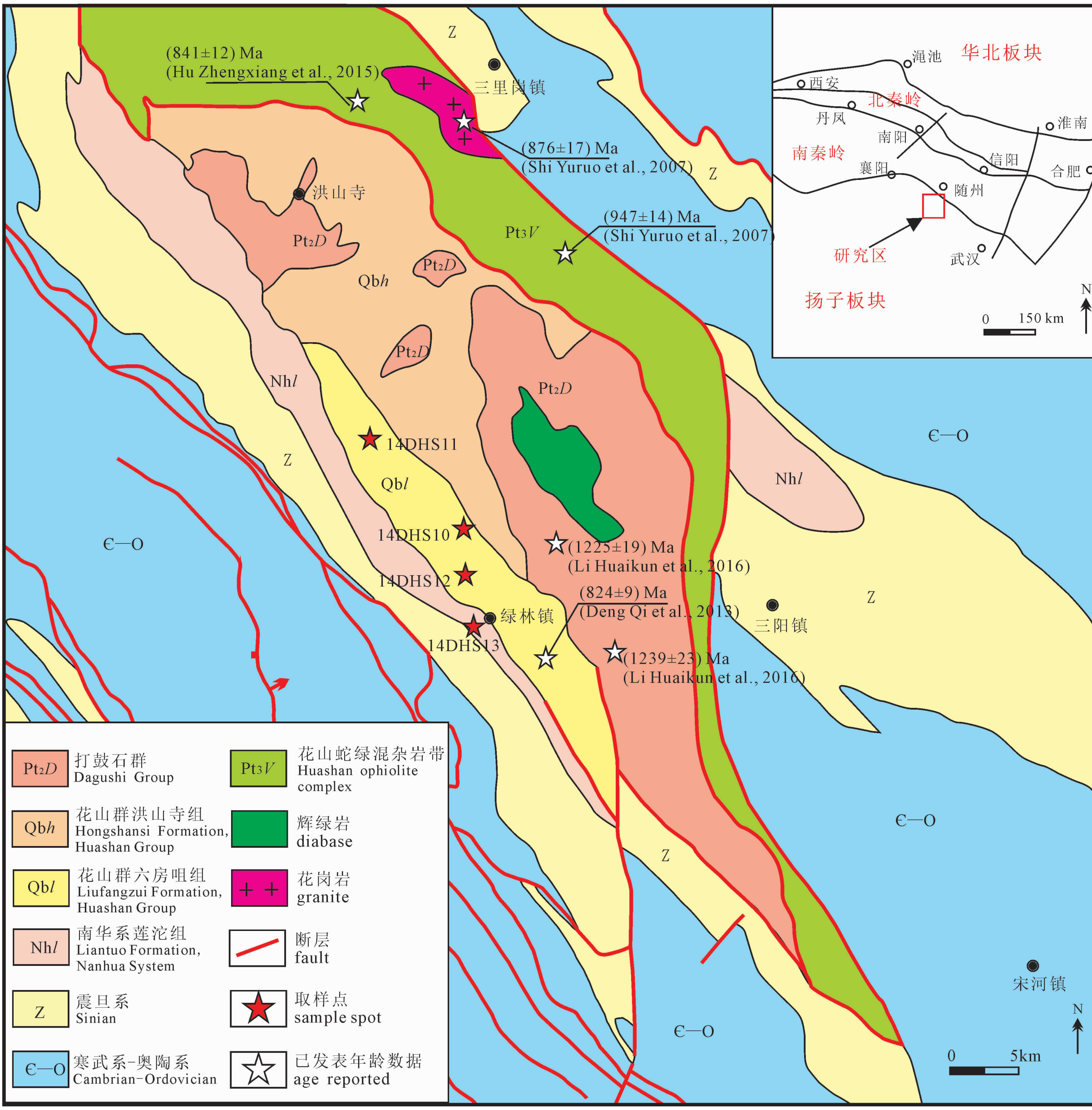

图 1　大洪山地区地质略图(据随州幅 1∶25 万建造构造图(湖北省地质调查院，未刊)修改)

Fig. 1　Geological sketch map of Dahongshan area (modified after 1∶250000 Formation-tectonic map of Suizhou, Hubei institute, Geological Survey, Unpublished)

岩带以西。花山群不整合覆盖于打鼓石群之上，顶部被南华系莲沱组不整合覆盖，东部与花山蛇绿混杂岩呈构造接触；总厚度 207～1252m，自下而上包括洪山寺组和六房咀组：① 洪山寺组为一套浅变质的粗碎屑沉积建造，主要包括灰色—灰白色中—厚层白云质砾岩(图 2a)、含砾岩屑长石砂岩夹黄绿色粉砂质-钙质板岩；② 六房咀组为一套浅变质细碎屑沉积建造，主要包括灰绿色—紫红色粉砂岩、黄绿色砂质板岩(图 2b)夹石英细砂岩、基性火山岩及凝灰岩；其中基性火山岩主要为深绿色玄武岩，局部发育较明显的枕状构造(图 2c)，具有大量方解石充填的杏仁体(图 2d)；凝灰岩主要为玄武质成分，具有熔结角砾(图 2e、f、g)。

花山群之下的打鼓石群为一套浅变质藻礁碳酸盐岩及砂、泥砂质碎屑岩组合，笔者等(2016)曾在打鼓石群中获得两层凝灰岩(取样点见图 1)，锆石 SHRIMP U-Pb 年龄 1225 ± 19 Ma 和 1239 ± 23 Ma(Li Huaikun et al.，2016)。花山群之上为南华系莲沱组，主要岩性为紫红色厚层状砾岩、含砾岩屑长石砂岩(图 2h)、岩屑砂岩和凝灰质砂岩等。

本文研究的样品包括花山群六房咀组玄武质熔结凝灰岩(14DHS10)、变质碎屑岩(14DHS11 和

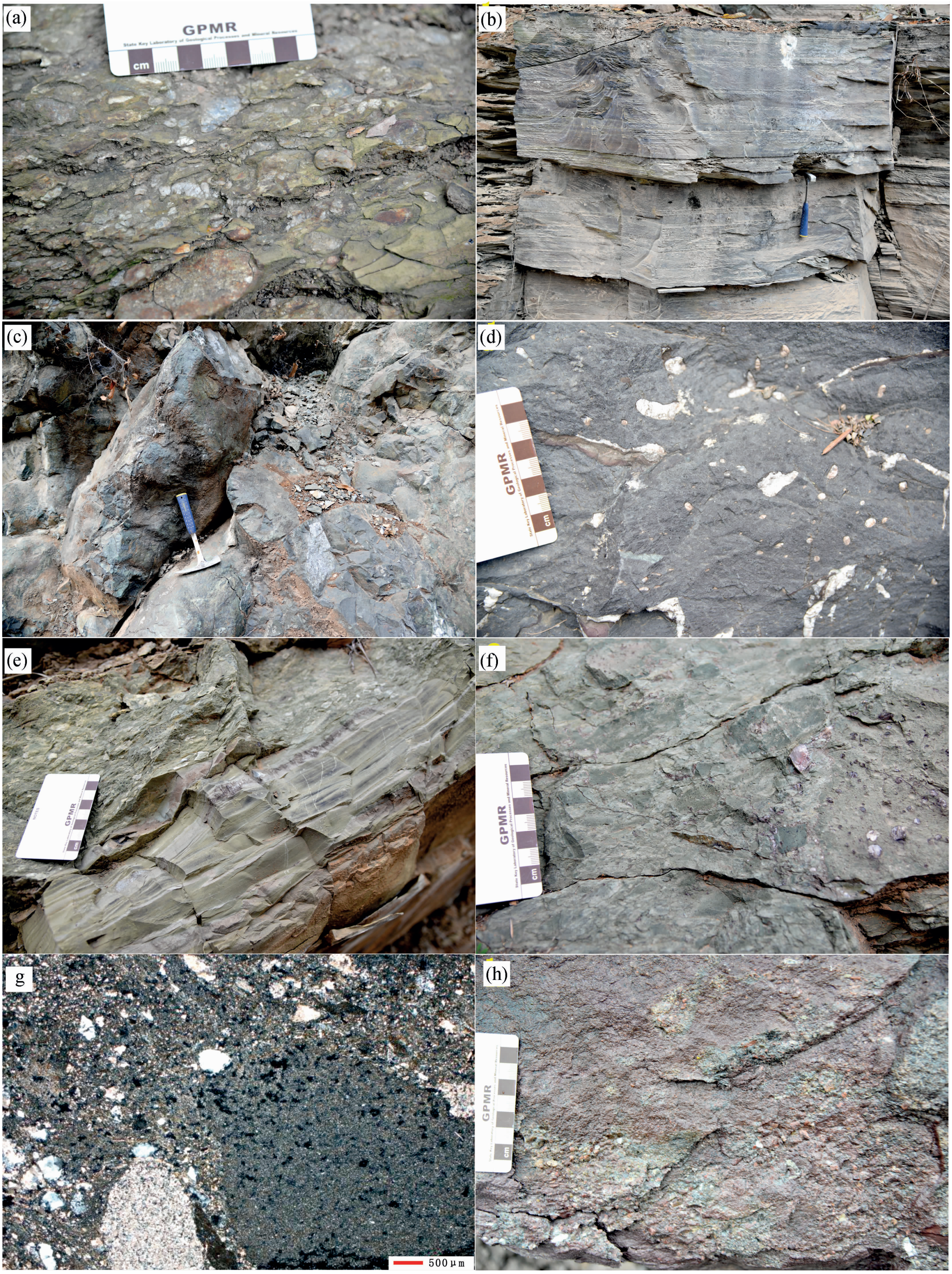

图 2　花山群及上覆地层莲沱组主体岩性的岩石学特征

Fig. 2　Petrographic characteristics of the main lithology in the Huashan Group and the overlying Liantuo Formation

(a)—花山群洪山寺组砾岩;(b)—花山群六房咀组砂质板岩;(c)—花山群六房咀组枕状玄武岩;(d)—枕状玄武岩中发育杏仁构造;(e)—花山群六房咀组底部细砂岩夹玄武质熔结凝灰岩;(f)—玄武质熔结凝灰岩中的火山角砾岩;(g)—玄武质熔结凝灰岩显微图像;(h)—南华系莲沱组含砾砂岩

(a)—Conglomerate in Hongshansi Formation, Huashan Group; (b)—sandy slate in Liufangzui Formation, Huashan Group; (c)—basaltic pillow-lava in Liufangzui Formation, Huashan Group; (d)—almond structure in pillow-lava; (e)—bassatic tuff within fine-sandstone at the bottom of Liufangzui Formation, Huashan Group; (f)—volcanic breccias in basaltic tuff; (g)—photomicrograph of basaltic tuff; (h)—conglomerate-sandstone in Liantuo Formation

14DHS12)，以及南华系莲沱组碎屑岩(14DHS13)，取样剖面位于洪山寺—绿林镇一带(图 1)，剖面中主要岩性特征如图 2 所示。

2　样品特征

(1)14DHS10 玄武质熔结(角砾)凝灰岩：产出于暗绿色中—薄层细砂岩之中(图 2e)，厚度约 30 cm，呈角砾状熔结凝灰结构，块状构造。岩石由火山碎屑物、蚀变新生矿物组成。火山碎屑物主要由火山角砾(45%左右)和凝灰物(55%左右)组成。火山角砾主要由刚性岩屑组成，呈团块状，杂乱分布，粒度 2～20 mm，成分可见玄武岩、黏土岩、杏仁状玄武岩等。凝灰物由火山尘、岩屑、晶屑和玻屑组成，玻屑、火山尘已脱玻呈隐晶状长英质，填隙状沿晶屑或岩屑间定向分布，玻屑外形已消失，是否为塑性玻屑无法确定；岩屑为刚性岩屑，呈团块状，杂乱分布，成分可见玄武岩、硅质岩、流纹岩、硅质白云岩等；晶屑由石英组成，呈棱角状，杂乱分布，粒度 0.05～0.9 mm；新生矿物为绢云母、绿泥石，呈鳞片状，粒度＜0.05 mm(图 2g)。所选锆石呈长柱状，长轴 50～200 μm，短轴 30～80 μm，具有典型基性岩浆锆石特征，CL 图像显示振荡环带宽缓不明晰(图 3)，Th/U 比值 0.73～1.4。

(2)14DHS11(变质)细粒岩屑砂岩：(变余)细粒砂状结构，板状构造，岩石由陆源砂(95%左右)和填隙物(5%左右)组成。陆源砂由石英、岩屑及少量长石组成，呈次棱角状，分选性好，磨圆度中等。所选锆石呈短柱状或椭圆状，长度 50～100 μm，磨圆度较好，锆石类型复杂，颜色深浅不一，CL 图像显示部分锆石振荡环带明显(图 3)，Th/U 比值多在 0.3～1.0 之间。

(3)14DHS12 绢云粉砂质板岩：变余泥质粉砂状结构，板状构造，岩石由陆源粉砂(55%左右)、绢云母(40%左右)及少量绿泥石(5%左右)组成。陆源粉砂由长石、石英组成。绢云母呈鳞片状，均匀定向分布；绿泥石呈鳞片状零星分布。所选锆石呈短柱状或椭圆状，长度 30～50 μm，磨圆度较好，锆石颜色深浅不一，形态、种类多样，CL 图像显示部分锆石振荡环带明显(图 3)，Th/U 比值多在 0.3～1.0 之间。

(4)14DHS13 含砾中粗粒长石岩屑砂岩：含砾中粗粒砂状结构，块状构造，主要由陆源碎屑(90%左右)、填隙物(10%左右)组成。陆源碎屑由长石、石英、岩屑组成，填隙物由黏土质组成。所选锆石呈短柱状或椭圆状，长度 100～300 μm，总体磨圆度较好，锆石颜色深浅不一，形态、种类多样，CL 图像显示部分锆石振荡环带明显(图 3)，Th/U 比值普遍在 0.3～1.5 之间。

3　测试方法及流程

玄武质熔结凝灰岩(14DHS10)锆石微区原位 U-Pb 同位素年龄测定在北京离子探针中心利用高灵敏度高分辨率离子探针质谱仪(SHRIMP Ⅱ)完成，详细分析流程及原理参见 Compston et al. (1984，1992)、Williams et al. (1998)及 Song Biao et al. (2002)。测试过程中采用标准锆石 TEM(Black et al.，2003)进行同位素分馏校正，使用标准锆石 M257 进行待测样品 U、Th 和 Pb 含量标定(Nasdala et al.，2008)。应用 SQUID 和 ISOPLOT 程序进行数据处理(Ludwig，2003a，2003b)，采用锆石样品中实际测得的 ^{204}Pb 进行普通 Pb 校正，数据表中所列单个数据点的误差为 1σ，加权平均年龄为 95% 的置信度。在具体测试过程中，每测定四个样品点进行一次标准锆石 TEM 测定，以监控仪器的稳定性及测定数据的有效性。

细粒岩屑砂岩、砂质板岩及含砾砂岩(14DHS11、14DHS12 和 14DHS13)的碎屑锆石利用天津地质矿产研究所同位素实验室的激光烧蚀多接收器电感耦合等离子体质谱仪(LA-MC-ICPMS)进行微区原位 U-Pb 同位素测定，详细分析流程及原理参见 Li Huaikun et al. (2009)、Hou Kejun et al. (2009)和 Geng Jianzhen et al. (2012)。在具体测试过程中，每测定八个样品点进行一次外部标准锆石(GJ-1)(Jackson et al.，2004)U-Pb 同位素测定，用以进行同位素分馏校正，以保证仪器的稳定性及测定数据的有效性；采用 Liu Yongsheng et al. (2010) ICPMS DataCal 程序和 Ludwig(2003a，2003b)的 Isoplot 程序进行数据处理，应用 ^{208}Pb 法进行普通铅校正(Anderson，2002)，通过测定 NIST610 玻璃标样计算锆石样品中的 Pb、U、Th 含量；数据表中所列单个数据点的误差为 1σ，加权平均年龄为 95%的置信度。

4　U-Pb 同位素测试结果

14DHS10(玄武质熔结凝灰岩)共测试 18 个 U-Pb 数据点，基本上所有点均落在谐和线上，^{206}Pb/^{238}U 表面年龄加权平均值为 814.7±7.3 Ma(n=18，MSWD=0.55)(图 4)；14DHS11((变

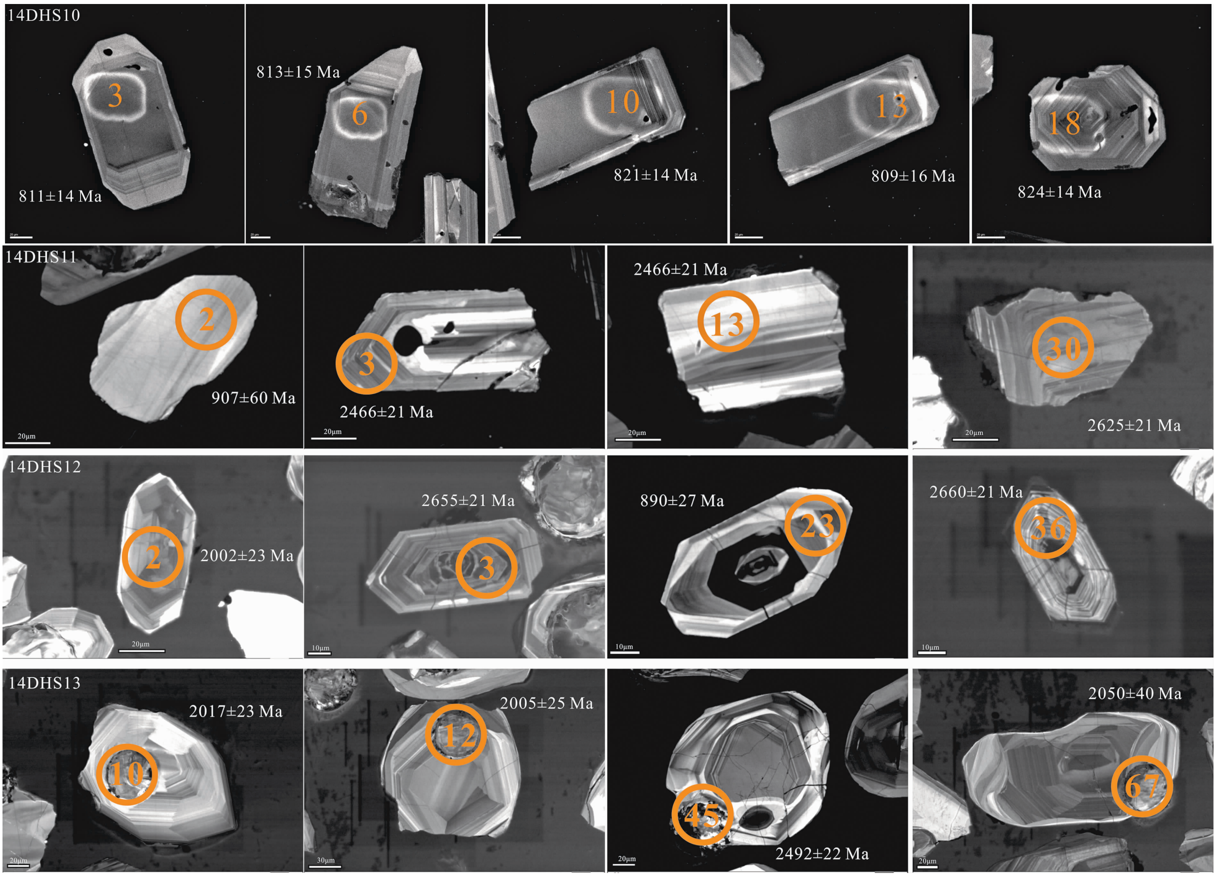

图 3 14DHS10、14DHS11、14DHS12、14DHS13 样品锆石阴极发光图像(CL)及测试点位

Fig. 3 Cathodoluminscene images and laser-ablated spots of zircons from sample 14DHS10, 14DHS11, 14DHS12 and 14DHS13

质)细粒岩屑砂岩)碎屑锆石 U-Pb 年龄谱范围 900～3300 Ma，主要年龄峰值为 2650 Ma 和 2050 Ma，2650 Ma 为最显著峰值，最年轻峰值为～900 Ma；14DHS12(绢云粉砂质板岩)碎屑锆石 U-Pb 年龄谱区间为 900～2900 Ma，主要年龄峰值为 2650 Ma、2050 Ma，以 2650 Ma 峰值最为显著，最年轻峰值为～900 Ma；14DHS13(含砾中粗粒长石岩屑砂岩)碎屑锆石 U-Pb 年龄谱范围 900～3300 Ma，在 900 Ma、2050 Ma 和 2500 Ma 处存在显著峰值，最年轻峰值为～900 Ma(图 4)。花山群碎屑锆石样品均存在 900 Ma 最小峰值，制约了花山群的最大形成年龄为 900 Ma(碎屑锆石 U-Pb 年龄频率分布图中使用的是谐和度为 90%～110% 的数据点的 $^{207}Pb/^{206}Pb$ 表面年龄，详细测试结果见表 1 和表 2)。

5 讨论

5.1 花山群厘定

花山蛇绿混杂岩：三里岗-三阳(襄樊-广济)主断裂带南侧蛇绿混杂岩带中基性岩浆锆石年龄为 947±14 Ma，而侵入到花山蛇绿混杂岩中的花岗岩年龄为 876±17 Ma(Shi Yuruo et al., 2007)，土门乡(三里岗镇)附近英安岩 LA-ICP-MS 锆石 U-Pb 为年龄 841±12 Ma(Hu Zhengxiang et al., 2015)(图 1)。这些年龄数据表明，三里岗-三阳主断裂附近花山蛇绿混杂岩带中基性岩浆岩的形成时代为晋宁期，说明其并非勉略带的东延。

花山群：厂河乡(绿林镇南)一带花山群枕状玄武岩 SHRIMP 锆石 U-Pb 年龄约 820 Ma(Deng Qi et al., 2013)，本文在绿林镇北部得到的玄武质熔结凝灰岩年龄为 814.7±7.3 Ma。

这表明，位于花山蛇绿混杂岩带西部，狭义的花山群之中的基性火山岩、火山碎屑岩年龄均在 820 Ma 左右，与花山蛇绿混杂岩带内的岩浆岩时代存在显著差别，将其归并到狭义的花山群是恰当的，即花山群应包括洪山寺组粗碎屑沉积、六房咀组细碎屑沉积和基性火山岩、基性火山碎屑岩，为一套沉积-火山建造。

表 1　14DHS10 样品锆石 SHRIMP U-Th-Pb 同位素分析结果

Table 1　SHRIMP U-Th-Pb isotope data of zircons from sample 14DHS10*

测试点	$^{206}Pb_c$ (%)	($\times10^{-6}$)			Th/U	$^{206}Pb/^{238}U$ 年龄(Ma)		$^{207}Pb/^{206}Pb$ 年龄(Ma)		谐和度	$^{207}Pb^*/^{206}Pb^*$	±%	$^{207}Pb^*/^{235}U$	±%	$^{206}Pb^*/^{238}U$	±%	误差相关系数
		^{206}Pb	U	Th													
1	0.15	3.28	29	23	0.85	808	±24	777	±140	104	0.0651	6.8	1.198	7.5	0.1335	3.2	0.42
2	0.35	16.4	143	160	1.15	802	±17	684	± 68	117	0.0623	3.2	1.138	3.9	0.1325	2.3	0.57
3	0.29	13.6	118	124	1.09	811	±14	802	± 51	101	0.0659	2.4	1.217	3.1	0.1340	1.9	0.63
4	0.30	5.8	50	36	0.73	808	±17	740	±130	109	0.0639	6.3	1.177	6.7	0.1335	2.3	0.34
5	0.00	9.95	85	48	0.59	828	±19	838	± 55	99	0.067	2.7	1.266	3.7	0.1370	2.5	0.68
6	0.51	10.8	93	104	1.16	813	±15	684	± 78	119	0.0623	3.6	1.155	4.2	0.1345	2.0	0.52
7	0.37	12.4	109	124	1.18	796	±15	788	± 81	101	0.0654	3.9	1.186	4.3	0.1314	2.0	0.42
8	0.19	13.6	120	119	1.03	802	±14	763	± 53	105	0.0647	2.5	1.180	3.1	0.1324	1.9	0.59
9	—	26	221	222	1.04	829	±14	818	± 34	101	0.0664	1.6	1.256	2.4	0.1373	1.8	0.75
10	0.48	17.5	149	118	0.82	821	±14	682	± 79	120	0.0622	3.7	1.166	4.1	0.1359	1.9	0.43
11	—	13.3	117	113	1.00	805	±14	830	± 56	97	0.0668	2.7	1.224	3.3	0.1330	1.9	0.57
12	0.55	11.1	95	130	1.41	812	±16	675	± 71	120	0.062	3.3	1.147	3.9	0.1342	2.1	0.53
13	0.39	7.7	67	65	1.01	809	±16	860	± 78	94	0.0677	3.7	1.249	4.3	0.1338	2.1	0.51
14	0.26	23.7	201	175	0.90	827	±22	804	± 45	103	0.0659	2.1	1.244	3.5	0.1369	2.8	0.80
15	—	13.3	113	91	0.83	830	±20	790	± 60	105	0.0655	2.8	1.241	3.8	0.1374	2.5	0.68
16	0.22	16.3	136	112	0.85	837	±15	765	± 63	109	0.0647	3.0	1.237	3.5	0.1386	1.9	0.52
17	0.30	14.4	125	118	0.98	809	±15	708	± 60	114	0.063	2.8	1.161	3.4	0.1337	1.9	0.57
18	0.53	18.8	160	216	1.40	824	±14	642	± 83	128	0.0611	3.9	1.148	4.3	0.1363	1.9	0.42

注：$^{206}Pb_c$—普通铅含量；$^{206}Pb^*$—放射成因铅含量；谐和度＝($^{206}Pb/^{238}U$)年龄/($^{207}Pb/^{206}$)年龄×100%；同位素比率通过^{204}Pb校正；误差为 1σ。

表 2　14DHS11、14DHS12、14DHS13 样品碎屑锆石 LA-MC-ICPMS U-Th-Pb 同位素分析结果

Table 2　LA-MC-ICPMS U-Th-Pb isotope data of detrital zircons from sample 14DHS11, 14DHS12 and 14DHS13

样品号	含量($\times10^{-6}$)		同位素原子比例							误差相关	表面年龄(Ma)						谐和度(%)
	Pb	U	$^{232}Th/^{238}U$	$^{206}Pb/^{238}U$	误差(%)	$^{207}Pb/^{235}U$	误差(%)	$^{207}Pb/^{206}Pb$	误差(%)		$^{206}Pb/^{238}U$	1σ	$^{207}Pb/^{235}U$	1σ	$^{207}Pb/^{206}Pb$	1σ	
14DHS11																	
1	48	122	1.0336	0.3291	1.04	5.1143	1.43	0.1127	1.27	0.51	1834	19	1838	26	1844	23	99
2	7	42	0.5185	0.1599	1.08	1.5276	3.01	0.0693	2.92	0.27	956	10	942	28	907	60	105
3	69	147	0.4593	0.4288	1.04	9.5163	1.42	0.1610	1.25	0.52	2300	24	2389	34	2466	21	93
4	78	225	0.5792	0.3167	1.05	4.8834	1.42	0.1118	1.24	0.53	1774	19	1799	26	1829	23	97
5	62	118	0.7958	0.4545	1.19	12.8450	1.53	0.2050	1.24	0.61	2415	29	2668	41	2866	20	84
6	204	598	0.1488	0.3340	1.03	6.5122	1.40	0.1414	1.24	0.52	1858	19	2048	29	2244	21	83
7	164	297	0.9792	0.4501	1.04	10.4493	1.41	0.1684	1.24	0.53	2396	25	2475	35	2542	21	94
8	50	87	0.7039	0.4856	1.19	12.6066	1.56	0.1883	1.25	0.62	2552	30	2651	41	2727	21	94
9	138	384	0.5216	0.3262	1.11	7.6015	1.52	0.1690	1.25	0.58	1820	20	2185	33	2548	21	71
10	137	297	0.7615	0.4091	1.06	9.5457	1.45	0.1692	1.25	0.54	2211	23	2392	35	2550	21	87
11	138	313	1.3048	0.3431	1.05	5.8816	1.42	0.1243	1.26	0.51	1902	20	1959	28	2019	22	94
12	105	214	0.5756	0.4410	1.07	10.8514	1.44	0.1785	1.25	0.54	2355	25	2510	36	2639	21	89
13	80	176	0.7933	0.3915	1.06	6.8269	1.42	0.1265	1.25	0.53	2130	23	2089	30	2050	22	104
14	170	719	1.1377	0.2090	1.17	4.7434	1.52	0.1646	1.24	0.60	1223	14	1775	27	2504	21	49
15	73	119	0.3922	0.5469	1.12	15.3279	1.48	0.2033	1.24	0.57	2812	31	2836	42	2853	20	99
16	30	86	0.9013	0.3076	1.08	7.2477	1.50	0.1709	1.27	0.56	1729	19	2142	32	2567	21	67
17	73	172	1.3438	0.3331	1.04	5.2771	1.42	0.1149	1.26	0.51	1854	19	1865	26	1878	23	99
18	50	113	0.3169	0.4043	1.23	9.8774	1.79	0.1772	1.34	0.66	2189	27	2423	43	2627	22	83
19	168	285	0.4960	0.5238	1.05	13.0662	1.43	0.1809	1.25	0.52	2715	29	2684	38	2661	21	102
20	37	91	0.7582	0.3492	1.49	10.0974	1.84	0.2097	1.29	0.72	1931	29	2444	45	2903	21	66
21	60	152	0.6770	0.3506	1.04	6.1643	1.43	0.1275	1.27	0.51	1937	20	1999	29	2064	22	94
22	34	152	0.4981	0.2159	1.08	2.4236	1.51	0.0814	1.34	0.51	1260	14	1250	19	1232	26	102
23	70	174	0.2305	0.3935	1.09	6.9308	1.47	0.1277	1.26	0.55	2139	23	2103	31	2067	22	103
24	35	218	0.6938	0.1464	1.10	1.4469	1.57	0.0717	1.35	0.54	881	10	909	14	977	27	90
25	119	206	0.4125	0.5171	1.09	12.8487	1.46	0.1802	1.24	0.56	2687	29	2669	39	2655	21	101

续表 2

样品号	含量($\times10^{-6}$)		同位素原子比例						误差相关	表面年龄(Ma)						谐和度(%)
	Pb	U	^{232}Th/^{238}U	^{206}Pb/^{238}U	误差(%)	^{207}Pb/^{235}U	误差(%)	^{207}Pb/^{206}Pb	误差(%)		^{206}Pb/^{238}U	1σ	^{207}Pb/^{235}U	1σ	^{207}Pb/^{206}Pb	1σ	
26	185	485	0.3454	0.3613	1.27	6.8778	1.59	0.1381	1.24	0.65	1988	25	2096	33	2203	22	90
27	87	299	1.1176	0.2559	1.75	4.5499	1.98	0.1289	1.25	0.78	1469	26	1740	35	2084	22	70
28	66	177	0.1100	0.3783	1.19	6.3766	1.54	0.1222	1.26	0.60	2068	25	2029	31	1989	22	104
29	68	103	1.0847	0.5214	1.41	13.2931	1.76	0.1849	1.26	0.71	2705	38	2701	48	2697	21	100
30	68	121	0.4068	0.5090	1.13	12.4229	1.52	0.1770	1.27	0.58	2653	30	2637	40	2625	21	101
31	109	219	0.5386	0.4504	1.28	9.4642	1.63	0.1524	1.26	0.65	2397	31	2384	39	2373	21	101
32	91	161	0.3887	0.5103	1.30	12.3923	1.65	0.1761	1.25	0.66	2658	35	2635	44	2617	21	102
33	118	229	0.6049	0.4614	1.04	11.2486	1.41	0.1768	1.24	0.52	2446	25	2544	36	2623	21	93
34	7	14	0.6319	0.4858	1.08	11.2978	1.87	0.1687	1.75	0.40	2553	28	2548	48	2544	29	100
35	2	8	0.6113	0.2529	1.56	5.9568	4.70	0.1708	4.63	0.21	1453	23	1970	93	2566	77	57
36	93	167	0.6259	0.4824	1.25	12.7245	1.62	0.1913	1.24	0.65	2538	32	2659	43	2754	20	92
37	62	114	0.4645	0.4849	1.17	12.3051	1.51	0.1840	1.25	0.60	2549	30	2628	40	2690	21	95
38	56	121	1.2543	0.3708	1.09	6.4530	1.49	0.1262	1.28	0.55	2033	22	2040	30	2046	23	99
39	63	139	0.8804	0.3891	1.05	6.9403	1.44	0.1294	1.26	0.52	2119	22	2104	30	2089	22	101
40	24	132	0.7534	0.1628	1.10	2.0300	1.77	0.0904	1.48	0.55	972	11	1126	20	1435	28	68
41	22	94	0.7417	0.2124	1.04	2.6769	1.57	0.0914	1.43	0.46	1241	13	1322	21	1456	27	85
42	3	13	0.6865	0.2273	1.29	3.4315	5.12	0.1095	5.02	0.20	1320	17	1512	77	1791	91	74
43	144	398	0.2946	0.3520	1.07	5.7948	1.45	0.1194	1.24	0.55	1944	21	1946	28	1947	22	100
44	57	114	0.3740	0.4586	1.06	10.7432	1.42	0.1699	1.26	0.52	2434	26	2501	36	2557	21	95
45	92	202	0.4463	0.4292	1.23	10.5763	1.57	0.1787	1.24	0.63	2302	28	2487	39	2641	21	87
46	23	59	1.1237	0.3279	1.05	5.3662	1.52	0.1187	1.36	0.49	1828	19	1879	29	1937	24	94
47	72	147	0.6962	0.4414	1.23	10.6417	1.57	0.1748	1.24	0.63	2357	29	2492	39	2605	21	91
48	89	168	0.5292	0.4747	1.07	11.7531	1.43	0.1796	1.24	0.54	2504	27	2585	37	2649	21	95
49	23	83	1.0233	0.2248	1.12	4.1796	1.52	0.1349	1.38	0.49	1307	15	1670	25	2162	24	60
50	101	180	0.4671	0.4981	1.31	12.4603	1.72	0.1814	1.26	0.68	2606	34	2640	45	2666	21	98
51	40	177	1.1234	0.2003	1.10	2.3600	1.53	0.0855	1.34	0.53	1177	13	1231	19	1326	26	89
52	135	497	1.3076	0.2260	1.94	4.5948	2.29	0.1475	1.25	0.84	1313	25	1748	40	2317	22	57
53	165	1012	1.1605	0.1451	1.24	2.2673	1.57	0.1133	1.24	0.63	873	11	1202	19	1853	22	47
54	94	211	0.5466	0.4069	1.25	7.6714	1.57	0.1368	1.25	0.63	2201	27	2193	34	2186	22	101
55	59	156	0.8169	0.3309	1.12	5.4739	1.61	0.1200	1.44	0.50	1843	21	1897	31	1956	26	94
56	112	402	0.2944	0.2654	1.19	4.2252	1.48	0.1155	1.29	0.56	1518	18	1679	25	1887	23	80
57	96	236	0.7080	0.3617	1.10	6.1386	1.48	0.1231	1.27	0.55	1990	22	1996	29	2002	23	99
58	329	1181	0.2412	0.2697	1.18	5.0684	1.62	0.1363	1.29	0.62	1539	18	1831	30	2181	22	71
59	82	154	0.4510	0.4841	1.11	11.9902	1.50	0.1796	1.29	0.54	2545	28	2604	39	2649	21	96
60	59	131	1.1782	0.3677	1.16	6.3601	1.55	0.1254	1.33	0.55	2019	23	2027	31	2035	23	99
61	23	77	0.5394	0.2744	1.10	4.2120	1.85	0.1113	1.62	0.50	1563	17	1676	31	1821	29	86
62	55	130	0.3706	0.4001	1.07	7.3332	1.48	0.1329	1.31	0.52	2170	23	2153	32	2137	23	102
63	15	44	0.7230	0.3122	1.07	4.8024	1.73	0.1116	1.61	0.42	1752	19	1785	31	1825	29	96
64	52	105	1.5979	0.3804	1.15	6.5948	1.54	0.1257	1.30	0.57	2078	24	2059	32	2039	23	102
65	121	234	0.9148	0.4657	1.18	11.5197	1.54	0.1794	1.26	0.59	2465	29	2566	39	2647	21	93
66	45	240	0.6470	0.1777	1.04	1.8332	1.48	0.0748	1.32	0.50	1055	11	1057	16	1063	27	99
67	97	174	0.3890	0.5100	1.17	12.7778	1.53	0.1817	1.26	0.59	2657	31	2663	41	2668	21	100
68	75	337	0.9327	0.2000	1.16	4.1238	1.60	0.1495	1.29	0.61	1175	14	1659	27	2341	22	50
69	42	139	0.8450	0.2763	1.33	4.8985	1.65	0.1286	1.30	0.64	1572	21	1802	30	2079	23	76
70	33	104	0.7429	0.2876	1.08	3.9946	1.55	0.1007	1.37	0.51	1630	18	1633	25	1638	25	100
71	134	298	1.0884	0.3885	1.05	8.2972	1.44	0.1549	1.28	0.50	2116	22	2264	33	2401	22	88
72	127	324	0.6172	0.3623	1.16	6.1461	1.53	0.1230	1.27	0.58	1993	23	1997	31	2001	23	100
73	93	256	0.8162	0.3229	1.12	4.4561	1.49	0.1001	1.27	0.56	1804	20	1723	26	1626	24	111
74	40	221	0.9049	0.1590	1.07	1.7845	1.61	0.0814	1.42	0.50	951	10	1040	17	1231	28	77
75	91	181	0.5288	0.4467	1.34	11.5105	1.70	0.1869	1.26	0.68	2380	32	2565	44	2715	21	88
76	55	147	0.9278	0.3157	1.09	5.7406	1.56	0.1319	1.32	0.55	1769	19	1937	30	2123	23	83
77	87	161	0.3405	0.4974	1.12	12.2824	1.49	0.1791	1.27	0.56	2602	29	2626	39	2645	21	98
78	176	522	0.7061	0.3085	1.33	5.4718	1.75	0.1286	1.29	0.68	1733	23	1896	33	2080	23	83

续表 2

样品号	含量(×10⁻⁶)		同位素原子比例						误差相关	表面年龄(Ma)						谐和度(%)
	Pb	U	$^{232}Th/^{238}U$	$^{206}Pb/^{238}U$	误差(%)	$^{207}Pb/^{235}U$	误差(%)	$^{207}Pb/^{206}Pb$	误差(%)		$^{206}Pb/^{238}U$	1σ	$^{207}Pb/^{235}U$	1σ	$^{207}Pb/^{206}Pb$	1σ	
79	61	314	0.6626	0.1799	1.05	1.9042	1.49	0.0767	1.36	0.47	1067	11	1083	16	1115	27	96
80	123	247	0.7710	0.4269	1.07	9.3588	1.47	0.1590	1.30	0.51	2292	24	2374	35	2445	22	94
81	123	247	0.7779	0.4257	1.07	9.3208	1.47	0.1588	1.30	0.51	2286	24	2370	35	2443	22	94
82	172	348	0.4245	0.4520	1.08	10.9293	1.46	0.1754	1.29	0.52	2404	26	2517	37	2610	21	92
83	79	174	0.6254	0.4064	1.05	9.7484	1.45	0.1740	1.28	0.51	2198	23	2411	35	2596	21	85
84	8	17	0.4056	0.3371	1.47	12.7378	2.32	0.2741	1.95	0.55	1873	28	2660	62	3329	31	56
85	56	147	0.9873	0.3332	1.07	7.1277	1.44	0.1551	1.26	0.52	1854	20	2128	31	2403	21	77
86	20	131	0.8475	0.1389	1.05	1.3370	1.71	0.0698	1.56	0.44	838	9	862	15	923	32	91
87	28	136	1.0571	0.1728	1.05	2.0598	1.54	0.0865	1.42	0.45	1027	11	1136	17	1349	27	76
88	87	239	0.7867	0.3265	1.02	5.4325	1.40	0.1207	1.25	0.51	1821	19	1890	27	1966	22	93
89	8	53	0.6073	0.1392	1.05	1.5652	2.59	0.0815	2.47	0.31	840	9	957	25	1235	48	68
90	120	234	0.3660	0.4718	1.06	11.4153	1.44	0.1755	1.25	0.53	2491	26	2558	37	2611	21	95
91	27	177	0.8993	0.1344	1.03	1.2901	1.63	0.0696	1.49	0.45	813	8	841	14	917	31	89
92	83	180	0.3114	0.4351	1.07	8.8862	1.45	0.1481	1.25	0.54	2328	25	2326	34	2325	22	100
93	75	94	0.4202	0.6743	1.09	24.8564	1.46	0.2674	1.25	0.55	3322	36	3303	48	3291	20	101
94	142	580	0.8189	0.2074	1.04	4.3721	1.62	0.1529	1.42	0.51	1215	13	1707	28	2378	24	51
95	140	316	0.4783	0.4022	2.06	9.9222	2.26	0.1789	1.24	0.84	2179	45	2428	55	2643	21	82
96	126	223	0.3722	0.4957	1.09	18.2787	1.45	0.2674	1.24	0.56	2595	28	3005	44	3291	19	79
97	3	7	0.8293	0.3080	1.75	9.0484	4.18	0.2131	4.12	0.24	1731	30	2343	98	2929	67	59
98	95	167	0.3132	0.5249	1.12	12.9533	1.48	0.1790	1.24	0.57	2720	31	2676	39	2644	21	103
99	60	76	1.5477	0.5794	1.10	16.8029	1.47	0.2103	1.26	0.56	2946	33	2924	43	2908	20	101
100	30	178	1.2796	0.1443	1.78	2.4213	2.29	0.1217	1.48	0.76	869	15	1249	29	1981	26	44
101	44	79	0.5647	0.5029	1.05	12.8086	1.45	0.1847	1.27	0.52	2626	28	2666	39	2696	21	97
102	55	80	1.5011	0.5157	1.15	12.9104	1.53	0.1816	1.29	0.57	2681	31	2673	41	2667	21	101
103	58	105	0.4414	0.4987	1.05	12.2503	1.43	0.1781	1.25	0.52	2608	27	2624	37	2636	21	99
104	68	179	1.4010	0.3353	1.06	8.1951	1.45	0.1772	1.26	0.53	1864	20	2253	33	2627	21	71
105	118	555	0.7164	0.1948	1.07	4.0991	1.46	0.1526	1.25	0.55	1147	12	1654	24	2376	21	48
106	9	47	0.8245	0.1741	1.47	3.6204	3.12	0.1508	3.08	0.26	1035	15	1554	48	2355	53	44
107	5	29	0.6849	0.1330	2.22	4.2317	3.11	0.2308	2.85	0.47	805	18	1680	52	3058	46	26
108	155	309	0.8291	0.4350	1.09	9.5305	1.44	0.1589	1.24	0.55	2328	25	2390	35	2444	21	95
109	13	26	0.9289	0.3796	1.56	11.8943	2.75	0.2272	2.40	0.50	2074	32	2596	71	3033	38	68
110	78	156	0.2492	0.4745	1.08	10.3355	1.47	0.1580	1.26	0.55	2503	27	2465	36	2434	21	103
111	77	159	0.3881	0.4372	1.28	10.4152	1.63	0.1728	1.26	0.65	2338	30	2472	40	2585	21	90
14DHS12																	
1	146	209	0.2924	0.5141	1.15	12.7798	1.52	0.1803	1.29	0.56	2674	31	2664	40	2656	21	101
2	200	402	0.3506	0.3754	1.08	6.3741	1.46	0.1231	1.28	0.53	2055	22	2029	30	2002	23	103
3	164	241	0.4745	0.5168	1.07	12.8457	1.45	0.1803	1.28	0.52	2686	29	2668	39	2655	21	101
4	105	1150	0.8736	0.0697	1.07	0.7932	1.46	0.0826	1.29	0.51	434	5	593	9	1259	25	34
5	132	851	0.8866	0.1180	1.07	1.0939	1.46	0.0672	1.29	0.52	719	8	750	11	846	27	85
6	106	521	0.4175	0.1531	1.10	1.5445	1.49	0.0731	1.29	0.54	919	10	948	14	1018	26	90
7	90	131	0.7310	0.5058	1.15	12.5451	1.52	0.1799	1.28	0.57	2639	30	2646	40	2652	21	100
8	204	417	0.6391	0.3698	1.07	8.0181	1.46	0.1573	1.28	0.53	2028	22	2233	33	2426	22	84
9	172	277	0.4264	0.4653	1.10	10.9882	1.48	0.1713	1.28	0.54	2463	27	2522	37	2570	21	96
10	178	350	0.6768	0.3625	1.21	8.5133	1.62	0.1703	1.29	0.61	1994	24	2287	37	2561	22	78
11	168	245	0.2958	0.5202	1.07	12.9330	1.46	0.1803	1.29	0.52	2700	29	2675	39	2656	21	102
12	55	262	0.6585	0.1694	1.07	2.1742	1.79	0.0931	1.63	0.44	1009	11	1173	21	1489	31	68
13	121	196	0.1933	0.4646	1.08	10.3162	1.47	0.1610	1.28	0.53	2460	27	2464	36	2467	22	100
14	81	162	0.5321	0.3785	1.08	6.6188	1.47	0.1268	1.29	0.52	2069	22	2062	30	2054	23	101
15	124	627	0.6748	0.1527	1.07	1.6188	1.49	0.0769	1.34	0.49	916	10	978	15	1119	27	82
16	111	149	0.3653	0.5540	1.13	15.3165	1.50	0.2005	1.28	0.56	2842	32	2835	42	2830	21	100
17	57	202	0.7010	0.2164	1.10	2.4855	1.52	0.0833	1.34	0.51	1263	14	1268	19	1277	26	99
18	66	359	0.6767	0.1384	1.12	1.5060	1.58	0.0789	1.38	0.52	836	9	933	15	1170	27	71
19	197	462	0.9274	0.3231	1.08	6.7080	1.48	0.1506	1.29	0.52	1805	19	2074	31	2352	22	77

续表 2

样品号	含量(×10^{-6})		同位素原子比例						误差相关	表面年龄(Ma)						谐和度(%)
	Pb	U	^{232}Th/^{238}U	^{206}Pb/^{238}U	误差(%)	^{207}Pb/^{235}U	误差(%)	^{207}Pb/^{206}Pb	误差(%)		^{206}Pb/^{238}U	1σ	^{207}Pb/^{235}U	1σ	^{207}Pb/^{206}Pb	1σ	
20	143	411	0.4868	0.2525	1.23	4.2361	1.58	0.1217	1.31	0.59	1451	18	1681	26	1981	23	73
21	163	288	0.7116	0.4264	1.09	9.7588	1.49	0.1660	1.30	0.53	2289	25	2412	36	2518	22	91
22	94	218	0.9079	0.3109	1.18	5.6192	1.65	0.1311	1.34	0.60	1745	21	1919	32	2112	24	83
23	70	371	0.7943	0.1439	1.07	1.3632	1.49	0.0687	1.33	0.50	867	9	873	13	890	27	97
24	109	271	0.6063	0.3064	1.07	4.6244	1.46	0.1095	1.29	0.52	1723	18	1754	26	1791	24	96
25	25	149	2.1660	0.1382	1.06	1.4377	1.89	0.0754	1.77	0.39	835	9	905	17	1080	35	77
26	114	171	0.5972	0.5028	1.09	12.8056	1.47	0.1847	1.27	0.54	2626	29	2665	39	2696	21	97
27	137	377	1.0737	0.2305	1.91	3.9562	2.20	0.1245	1.28	0.82	1337	26	1625	36	2022	23	66
28	74	447	1.0214	0.1154	1.40	1.2262	1.73	0.0771	1.35	0.65	704	10	813	14	1124	27	63
29	94	184	0.9040	0.3844	1.10	8.1698	1.47	0.1542	1.28	0.53	2097	23	2250	33	2393	22	88
30	76	171	0.9665	0.3387	1.06	5.9892	1.49	0.1282	1.30	0.52	1880	20	1974	29	2074	23	91
31	277	742	0.4115	0.2815	1.09	7.7806	1.46	0.2004	1.28	0.53	1599	17	2206	32	2830	21	57
32	217	480	0.7059	0.3058	1.41	5.9466	1.78	0.1411	1.28	0.70	1720	24	1968	35	2240	22	77
33	96	354	1.4602	0.1919	1.24	3.9348	1.61	0.1487	1.28	0.62	1131	14	1621	26	2331	22	49
34	35	191	0.6028	0.1433	1.05	1.6331	1.60	0.0827	1.46	0.46	863	9	983	16	1261	28	68
35	11	62	1.2564	0.1388	1.10	2.2227	2.08	0.1161	1.90	0.43	838	9	1188	25	1898	34	44
36	114	161	0.3893	0.5129	1.17	12.7823	1.52	0.1807	1.27	0.58	2669	31	2664	41	2660	21	100
37	36	192	1.5227	0.1492	1.07	1.4534	1.57	0.0707	1.43	0.47	896	10	911	14	947	29	95
38	53	379	1.2111	0.1063	1.07	1.1802	1.59	0.0805	1.39	0.51	651	7	791	13	1209	27	54
39	31	187	1.2080	0.1360	1.07	1.3752	1.67	0.0734	1.56	0.42	822	9	878	15	1024	32	80
40	158	278	0.9273	0.4108	1.20	9.2260	1.56	0.1629	1.28	0.60	2219	27	2361	37	2486	22	89
14DHS13																	
1	30	49	0.6274	0.5179	1.20	13.0535	1.63	0.1828	1.36	0.58	2690	32	2684	44	2678	22	100
2	128	234	0.6209	0.4838	1.11	10.8653	1.53	0.1629	1.29	0.56	2544	28	2512	38	2486	22	102
3	14	84	0.9160	0.1459	1.06	1.3157	2.75	0.0654	2.65	0.28	878	9	853	23	787	56	112
4	166	556	0.4017	0.2751	1.08	5.2438	1.50	0.1383	1.29	0.55	1566	17	1860	28	2206	22	71
5	136	249	0.7723	0.4793	1.12	11.1988	1.51	0.1695	1.28	0.56	2524	28	2540	38	2552	21	99
6	50	104	1.0964	0.3801	1.17	6.4702	1.63	0.1235	1.39	0.55	2077	24	2042	33	2007	25	103
7	70	137	0.2827	0.4739	1.08	10.8108	1.53	0.1655	1.30	0.54	2501	27	2507	38	2512	22	100
8	142	234	0.7300	0.5005	1.09	12.1047	1.50	0.1754	1.28	0.55	2616	29	2613	39	2610	21	100
9	115	212	0.4771	0.4796	1.09	10.5943	1.50	0.1602	1.29	0.54	2526	28	2488	37	2458	22	103
10	75	168	0.8522	0.3874	1.04	6.6335	1.48	0.1242	1.30	0.51	2111	22	2064	31	2017	23	105
11	102	228	0.7903	0.3806	1.14	6.5023	1.55	0.1239	1.29	0.57	2079	24	2046	32	2013	23	103
12	40	80	1.2656	0.3786	1.09	6.4377	1.59	0.1233	1.41	0.50	2070	23	2037	32	2005	25	103
13	80	155	1.3760	0.3827	1.05	6.6130	1.48	0.1253	1.30	0.52	2089	22	2061	31	2033	23	103
14	48	102	1.0461	0.3834	1.08	6.5694	1.52	0.1243	1.31	0.53	2092	23	2055	31	2018	23	104
15	19	98	1.3442	0.1481	1.05	1.3795	1.99	0.0676	1.84	0.40	890	9	880	18	856	38	104
16	81	201	0.6112	0.3570	1.07	7.4733	1.51	0.1518	1.30	0.54	1968	21	2170	33	2366	22	83
17	48	97	1.9095	0.3646	1.06	6.4552	1.50	0.1284	1.32	0.51	2004	21	2040	31	2076	23	97
18	131	163	0.3169	0.6844	1.14	25.6513	1.55	0.2718	1.29	0.57	3361	38	3333	52	3317	20	101
19	180	427	0.9968	0.3354	1.04	5.9605	1.48	0.1289	1.31	0.51	1865	19	1970	29	2083	23	90
20	64	143	0.7268	0.3687	1.16	6.5684	1.63	0.1292	1.36	0.57	2023	23	2055	33	2087	24	97
21	37	78	0.9890	0.3655	1.13	6.6469	1.67	0.1319	1.45	0.53	2008	23	2066	35	2123	25	95
22	106	243	0.7785	0.3607	1.06	6.2861	1.49	0.1264	1.30	0.52	1985	21	2017	30	2049	23	97
23	119	252	0.9238	0.3783	1.06	6.5384	1.50	0.1254	1.30	0.53	2068	22	2051	31	2034	23	102
24	43	95	0.7341	0.3786	1.07	6.7396	1.53	0.1291	1.33	0.52	2070	22	2078	32	2086	23	99
25	114	252	0.7926	0.3751	1.16	6.5508	1.56	0.1267	1.29	0.58	2053	24	2053	32	2052	23	100
26	50	111	0.8779	0.3685	1.06	6.3284	1.51	0.1245	1.32	0.52	2023	21	2022	31	2022	23	100
27	71	150	0.9459	0.3802	1.07	6.5510	1.50	0.1250	1.30	0.54	2077	22	2053	31	2028	23	102
28	56	122	0.9664	0.3633	1.07	6.2795	1.53	0.1254	1.31	0.54	1998	21	2016	31	2034	23	98
29	57	128	0.7227	0.3731	1.12	6.4736	1.56	0.1258	1.31	0.56	2044	23	2042	32	2041	23	100
30	23	130	1.0119	0.1430	1.07	1.3741	2.12	0.0697	1.93	0.42	861	9	878	19	920	40	94
31	125	203	0.5290	0.5216	1.17	13.2340	1.58	0.1840	1.30	0.59	2706	32	2696	43	2689	21	101

续表 2

样品号	含量(×10^{-6})		同位素原子比例							误差相关	表面年龄(Ma)						谐和度(%)
	Pb	U	^{232}Th/^{238}U	^{206}Pb/^{238}U	误差(%)	^{207}Pb/^{235}U	误差(%)	^{207}Pb/^{206}Pb	误差(%)		^{206}Pb/^{238}U	1σ	^{207}Pb/^{235}U	1σ	^{207}Pb/^{206}Pb	1σ	
32	18	36	1.6062	0.4079	1.13	7.5977	1.74	0.1351	1.53	0.50	2205	25	2185	38	2165	27	102
33	72	132	0.4968	0.4710	1.15	10.7078	1.56	0.1649	1.31	0.57	2488	29	2498	39	2506	22	99
34	120	274	0.6472	0.3792	1.18	6.5002	1.57	0.1243	1.29	0.59	2073	24	2046	32	2019	23	103
35	129	269	0.9564	0.3788	1.10	6.4958	1.52	0.1244	1.29	0.56	2070	23	2045	31	2020	23	102
36	111	200	0.5612	0.4751	1.08	10.7522	1.50	0.1641	1.28	0.55	2506	27	2502	38	2499	22	100
37	110	252	1.0080	0.3474	1.06	6.0208	1.49	0.1257	1.29	0.53	1922	20	1979	29	2039	23	94
38	60	137	0.6668	0.3709	1.08	6.3311	1.51	0.1238	1.30	0.53	2034	22	2023	30	2012	23	101
39	35	77	0.8922	0.3677	1.09	6.3234	1.55	0.1247	1.34	0.53	2019	22	2022	31	2025	24	100
40	61	131	0.9329	0.3755	1.09	6.3113	1.53	0.1219	1.31	0.54	2055	22	2020	31	1984	23	104
41	15	32	0.7253	0.3740	1.07	6.5797	1.72	0.1276	1.56	0.45	2048	22	2057	35	2065	28	99
42	48	110	0.6629	0.3765	1.07	6.4025	1.51	0.1233	1.31	0.53	2060	22	2033	31	2005	23	103
43	135	542	1.4722	0.1775	1.21	4.8697	1.52	0.1990	1.32	0.55	1053	13	1797	27	2818	22	37
44	76	132	0.7709	0.4727	1.20	10.6332	1.59	0.1631	1.29	0.60	2495	30	2492	40	2489	22	100
45	103	193	0.5495	0.4750	1.15	10.7054	1.55	0.1635	1.28	0.58	2505	29	2498	39	2492	22	101
46	17	98	0.7428	0.1482	1.25	1.3002	2.45	0.0636	2.15	0.48	891	11	846	21	729	46	122
47	40	77	1.4803	0.4108	1.03	7.1138	1.57	0.1256	1.39	0.49	2219	23	2126	33	2037	25	109
48	213	407	0.3542	0.4689	1.31	10.4921	1.67	0.1623	1.28	0.65	2479	32	2479	42	2480	22	100
49	59	141	0.7894	0.3488	1.11	6.0060	1.56	0.1249	1.31	0.56	1929	21	1977	31	2027	23	95
50	52	108	1.2608	0.3717	1.12	6.3283	1.59	0.1235	1.35	0.55	2038	23	2022	32	2007	24	102
51	130	231	0.5428	0.4906	1.20	11.6093	1.60	0.1716	1.30	0.60	2573	31	2573	41	2574	22	100
52	240	660	0.3901	0.3343	1.06	6.9124	1.48	0.1500	1.29	0.53	1859	20	2100	31	2345	22	79
53	38	194	1.2923	0.1522	1.09	1.3696	1.67	0.0653	1.51	0.47	913	10	876	15	783	32	117
54	9	56	0.7382	0.1486	1.27	1.3882	3.49	0.0677	3.37	0.27	893	11	884	31	861	70	104
55	293	645	0.5708	0.4004	1.04	8.6032	1.46	0.1558	1.28	0.52	2171	23	2297	34	2411	22	90
56	37	73	1.3373	0.3803	1.30	6.6627	1.72	0.1271	1.44	0.58	2078	27	2068	36	2058	25	101
57	26	146	0.8145	0.1528	1.25	1.5261	2.32	0.0724	2.06	0.47	917	11	941	22	999	42	92
58	99	179	0.5570	0.4807	1.33	10.8114	1.70	0.1631	1.29	0.66	2530	34	2507	43	2488	22	102
59	42	84	1.2101	0.3831	1.27	6.7342	1.67	0.1275	1.37	0.60	2091	27	2077	35	2064	24	101
60	65	124	1.4929	0.3834	1.24	6.6364	1.63	0.1255	1.32	0.61	2092	26	2064	34	2036	23	103
61	48	110	0.6432	0.3787	1.38	6.4964	1.79	0.1244	1.38	0.65	2070	29	2045	37	2020	25	102
62	146	320	0.5095	0.4211	1.04	8.9974	1.48	0.1550	1.29	0.52	2265	24	2338	34	2402	22	94
63	26	50	1.3291	0.4117	1.13	7.8146	1.66	0.1377	1.40	0.56	2222	25	2210	37	2198	24	101
64	65	124	0.5922	0.4530	1.07	10.2265	1.51	0.1637	1.30	0.54	2409	26	2455	37	2495	22	97
65	41	89	0.9342	0.3796	1.12	6.5372	1.56	0.1249	1.32	0.55	2074	23	2051	32	2028	23	102
66	52	111	1.1488	0.3691	1.06	6.3050	1.51	0.1239	1.32	0.52	2025	21	2019	31	2013	23	101
67	29	54	1.5284	0.3878	1.06	6.7636	2.38	0.1265	2.25	0.34	2113	22	2081	49	2050	40	103
68	57	120	1.3735	0.3587	1.11	6.1536	1.59	0.1244	1.36	0.54	1976	22	1998	32	2020	24	98
69	22	128	0.8786	0.1448	1.06	1.3349	2.34	0.0669	2.18	0.37	872	9	861	20	833	46	105
70	147	321	0.4591	0.4149	1.08	9.1865	1.57	0.1606	1.35	0.53	2237	24	2357	37	2462	23	91
71	104	261	0.8326	0.3340	1.04	5.6263	1.53	0.1222	1.36	0.49	1858	19	1920	29	1988	24	93
72	24	60	0.7337	0.3401	1.04	5.7192	1.63	0.1220	1.47	0.46	1887	20	1934	32	1985	26	95
73	40	87	1.0341	0.3760	1.12	6.3260	1.59	0.1220	1.36	0.54	2057	23	2022	32	1986	24	104
74	149	344	1.2569	0.3518	1.07	6.0155	1.52	0.1240	1.31	0.53	1943	21	1978	30	2015	23	96
75	16	30	1.7151	0.3837	1.08	6.5928	1.78	0.1246	1.62	0.45	2094	23	2058	37	2023	29	103
76	23	144	0.4940	0.1542	1.07	1.4675	1.84	0.0690	1.67	0.44	924	10	917	17	899	34	103
77	19	73	6.2122	0.1507	1.09	1.5230	2.37	0.0733	2.18	0.40	905	10	940	22	1022	44	89
78	25	120	1.9288	0.1476	1.06	1.3764	1.94	0.0676	1.79	0.41	888	9	879	17	857	37	104
79	59	121	1.2217	0.3884	1.08	6.4877	1.54	0.1211	1.33	0.53	2115	23	2044	31	1973	24	107
80	54	119	0.8819	0.3891	1.10	6.4462	1.57	0.1201	1.35	0.54	2119	23	2039	32	1958	24	108
81	55	119	0.8749	0.3917	1.10	6.7889	1.57	0.1257	1.35	0.54	2131	24	2084	33	2039	24	105
82	42	94	1.0779	0.3559	1.03	6.0830	1.53	0.1240	1.36	0.50	1963	20	1988	30	2014	24	97
83	68	145	1.0351	0.3783	1.08	6.6165	1.53	0.1269	1.33	0.53	2068	22	2062	32	2055	23	101
84	33	74	1.0886	0.3582	1.07	6.1453	1.57	0.1244	1.36	0.52	1974	21	1997	31	2021	24	98

续表 2

样品号	含量(×10⁻⁶)		同位素原子比例							误差相关	表面年龄(Ma)						谐和度(%)
	Pb	U	$^{232}Th/^{238}U$	$^{206}Pb/^{238}U$	误差(%)	$^{207}Pb/^{235}U$	误差(%)	$^{207}Pb/^{206}Pb$	误差(%)		$^{206}Pb/^{238}U$	1σ	$^{207}Pb/^{235}U$	1σ	$^{207}Pb/^{206}Pb$	1σ	
85	391	611	0.5016	0.5559	1.06	16.2401	1.49	0.2119	1.29	0.53	2850	30	2891	43	2920	21	98
86	115	269	1.0388	0.3795	1.07	8.0161	1.50	0.1532	1.29	0.54	2074	22	2233	34	2382	22	87
87	98	181	0.6245	0.4785	1.05	10.8146	1.48	0.1639	1.29	0.52	2521	26	2507	37	2496	22	101
88	130	246	0.5585	0.4686	1.06	10.5042	1.49	0.1626	1.29	0.53	2478	26	2480	37	2482	22	100
89	57	96	0.5562	0.5198	1.13	13.1777	1.57	0.1839	1.31	0.57	2698	31	2692	42	2688	22	100
90	64	155	0.7421	0.3632	1.04	6.2462	1.49	0.1247	1.31	0.51	1997	21	2011	30	2025	23	99
91	44	97	0.8723	0.3758	1.05	6.4716	1.55	0.1249	1.36	0.51	2057	22	2042	32	2027	24	101
92	65	136	1.3245	0.3696	1.04	6.3447	1.49	0.1245	1.32	0.51	2028	21	2025	30	2022	23	100
93	21	118	1.1554	0.1448	1.04	1.3680	2.02	0.0685	1.85	0.41	872	9	875	18	884	38	99
94	67	119	0.6687	0.4798	1.08	10.7018	1.50	0.1618	1.30	0.53	2526	27	2498	38	2474	22	102
95	10	60	0.6169	0.1525	1.12	1.3709	3.10	0.0652	3.03	0.24	915	10	877	27	781	64	117
96	51	89	0.6990	0.4856	1.08	10.7051	1.51	0.1599	1.31	0.53	2551	28	2498	38	2455	22	104
97	17	88	1.4052	0.1499	1.05	1.4339	2.70	0.0694	2.57	0.32	901	9	903	24	910	53	99
98	72	164	0.9360	0.3623	1.18	6.1034	1.57	0.1222	1.30	0.58	1993	24	1991	31	1988	23	100
99	128	196	1.0483	0.5057	1.15	12.4311	1.54	0.1783	1.29	0.58	2638	30	2638	41	2637	21	100
100	217	388	0.3386	0.5084	1.09	12.5484	1.51	0.1790	1.29	0.55	2650	29	2646	40	2644	21	100
101	20	118	0.7398	0.1515	1.13	1.4867	1.92	0.0712	1.77	0.42	909	10	925	18	962	36	95
102	45	102	0.7763	0.3745	1.14	6.4242	1.61	0.1244	1.39	0.53	2050	23	2036	33	2021	25	101
103	71	130	0.7583	0.4853	1.05	11.1012	1.69	0.1659	1.54	0.45	2550	27	2532	43	2517	26	101
104	10	53	1.4713	0.1512	1.06	1.5411	3.03	0.0739	2.90	0.30	908	10	947	29	1039	58	87
105	47	104	1.0078	0.3690	1.12	6.3541	1.56	0.1249	1.31	0.57	2025	23	2026	32	2027	23	100
106	58	118	1.6135	0.3590	1.11	6.0855	1.54	0.1229	1.31	0.55	1978	22	1988	31	1999	23	99
107	270	878	0.6689	0.2722	1.33	4.7110	1.67	0.1255	1.28	0.66	1552	21	1769	30	2036	23	76
108	20	42	0.8860	0.4013	1.11	7.7021	1.75	0.1392	1.51	0.52	2175	24	2197	38	2217	26	98
109	12	71	0.6838	0.1502	1.08	1.4381	2.27	0.0694	2.14	0.35	902	10	905	21	911	44	99
110	116	262	0.6071	0.4048	1.23	9.2884	1.60	0.1664	1.29	0.61	2191	27	2367	38	2522	22	87
111	65	129	0.5534	0.4544	1.09	10.2149	1.51	0.1630	1.31	0.54	2415	26	2454	37	2487	22	97

注:Pb 为锆石中全铅含量;同位素比率已采用^{208}Pb校正法进行了普通铅校正;表面年龄谐和度=($^{206}Pb/^{238}U$)年龄/($^{207}Pb/^{206}$)年龄×100;误差为 1σ。

5.2 花山群的沉积时代

本文两件花山群碎屑岩样品(4DHS11 和 14DHS12)最年轻锆石 U-Pb 年龄峰值均为 900 Ma,限定了其沉积年龄应小于 900 Ma;花山群六房咀组细砂岩中的玄武质熔结凝灰岩夹层(14DHS10)的锆石 U-Pb 同位素为 814.7±7.3 Ma,直接标定了花山群的沉积时代,而且 Deng Qi et al.(2013)和 Hu Zhengxiang et al.(2015)在绿林镇一带也获得约 820 Ma 玄武岩锆石 U-Pb 年龄数据。另外,花山群上覆的南华系莲沱组碎屑锆石(14DHS13)年龄信息与上述花山群数据亦不相悖,虽然有学者曾认为大洪山地区花山群上覆的莲沱组地层是晚侏罗世的产物(Li Jinyi et al.,2002),但本文中莲沱组碎屑锆石年龄值与华南地区莲沱组最新碎屑锆石研究成果(Zhang Xiong et al.,2016;Song Fang et al.,2016)相吻合,可确定为南华纪裂谷沉积物。

综合本文获得的花山群中玄武质熔结凝灰岩和碎屑岩锆石 U-Pb 年龄资料,加之其下伏打鼓石群(~1220 Ma Li Huaikun et al.,2016)和上覆南华系年龄限定,推断花山群沉积时代为 900 Ma 之后,大约在 815 Ma 前后快速沉积;结合前人在花山蛇绿混杂岩带中获得的年龄(840~950 Ma)(Shi Yuruo et al.,2007;Hu Zhengxiang et al.,2015),可以进一步推测,840~815 Ma 之间经历了一次挤压—伸展构造机制的转换,花山群很可能是在完成伸展转换之后开始沉积的。结合前人年代学资料和区域构造成果分析,花山群很可能形成于 820~815Ma。

5.3 花山群的物源特征

本文研究的花山群碎屑岩(14DHS11 和 14DHS12)具有相似的锆石 U-Pb 年龄谱,均出现的几个明显峰值为~2650 Ma、~2050 Ma 和~900 Ma,这些峰值在扬子板块碎屑锆石年龄谱(Wang Xiaolei et al.,2007;Sun Weihua et al.,2009;Xie Shiwen et al.,2009;Zhang Xiong et al.,2016)中均有出现(图 5),前两个年龄峰值与扬子板块北缘神

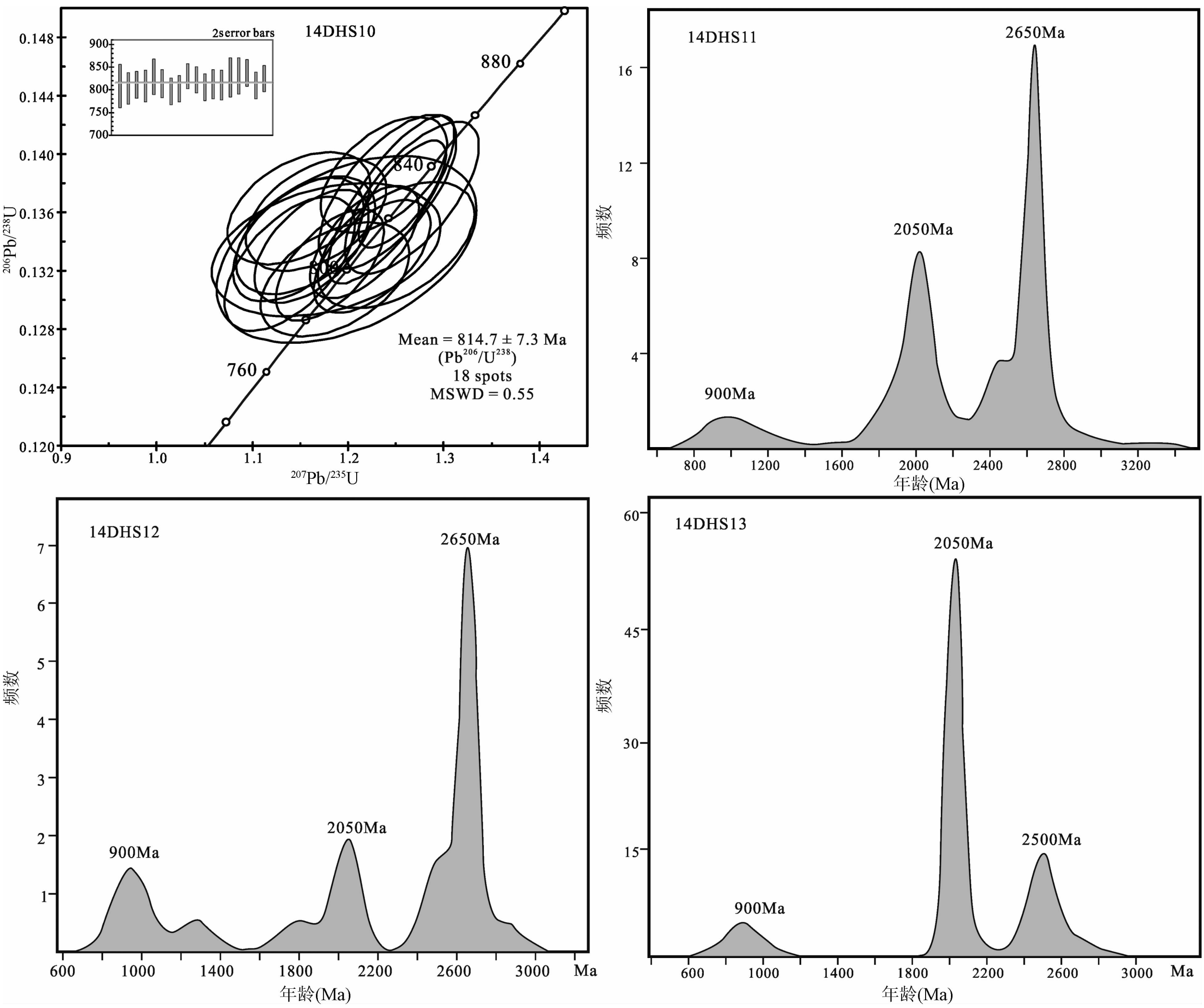

图 4　14DHS10 锆石 U-Pb 同位素谐和图，14DHS11、14DHS12 和 14DHS13 碎屑锆石 U-Pb 同位素年龄频率分布图

Fig. 4　SHRIMP zircon U-Pb concodia diagram for sample 14DHS10 and probability distribution diagrams of LA-MC-ICPMS detrital zircon U-Pb ages for sample 14DHS11, 14DHS12 and 14DHS13

农架地区神农架群(Li Huaikun et al.,2013)，以及郑家垭组碎屑锆石年龄峰值(Xu Daliang et al.,2016)一致(图 5)，而神农架群在大洪山地区的对应地层为打鼓石群(Li Huaikun et al.,2016)，而且野外调查发现花山群洪山寺组白云质砾石成分多来自打鼓石群，推测下伏打鼓石群是花山群的直接物源之一。碎屑锆石年龄谱中约 900 Ma 的峰值指示其物源区有 Rodinia 超大陆事件的信息；约 2050 Ma 的锆石年龄峰值可能代表崆岭杂岩在古元古代经历的构造热事件和扬子板块北缘古元古代的地壳再造事件(Zheng Yongfei and Zhang Shaobing,2007)。

新太古代约 2650 的年龄信息则指示花山群沉积物源区可能有来自扬子板块较古老的基底岩石——崆岭杂岩、黄土岭麻粒岩、鱼洞子杂岩以及后河杂岩等，这些古老地质记录中有约 2.7Ga 的锆石年龄信息(Zhao Guochun et al.,2012；Zhang Zongqing et al.,2001)。Zhang Zongqing et al.(2001)在扬子北缘碧口地区鱼洞子杂岩(群)中测得 2688±10 Ma 的 Sm-Nd 等时线年龄和 2693±9 Ma 花岗岩岩浆锆石上交点年龄。花山群在～2650 Ma 最突出的年龄峰值表明其源区可能与鱼洞子杂岩(群)相关。

5.4　花山群沉积构造背景

对于花山群形成的大地构造背景有不同的观点，Hu Zhengxiang et al.(2015)认为其属于俯冲增生杂岩的一部分，形成于岛弧背景；Deng Qi et al.(2013)认为花山群形成于大陆裂谷而不是岛弧或洋盆。

花山群中发育大量玄武质火山岩，地球化学特征一致表现为：低钾高钠，均属于拉斑系列；轻稀土

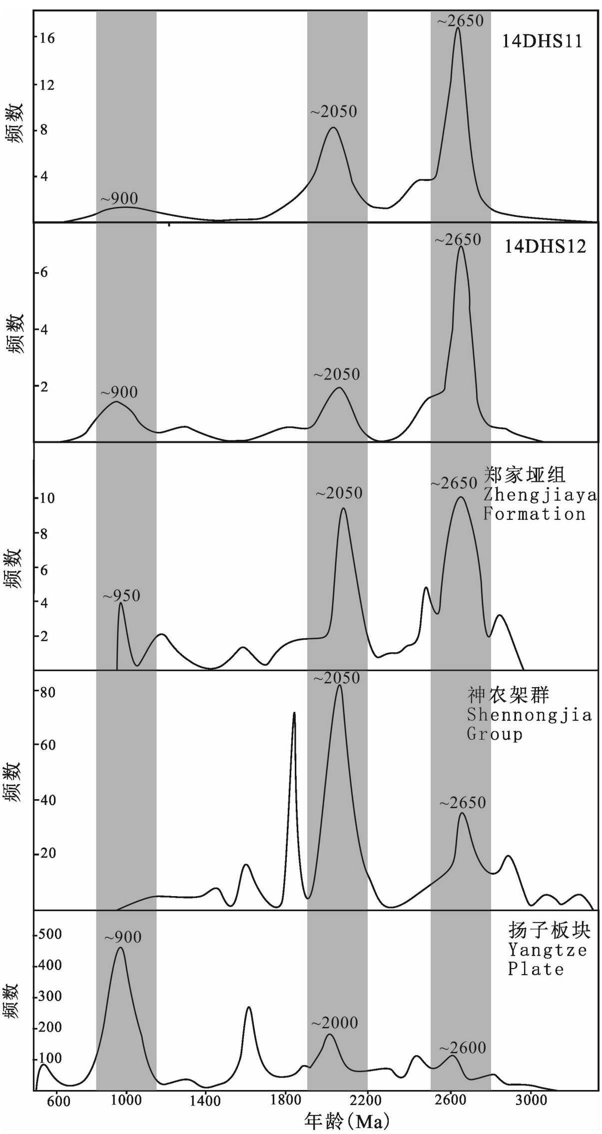

图 5 大洪山地区花山群与扬子板块其他地区碎屑锆石年龄对比

Fig. 5 Comparison of detrital zircon age spectra between Huashan Group in Dahongshan area and adjacent areas in the Yangtze plate

年龄数据来源:神农架群,Li Huaikun et al.,2013;郑家垭组,Xu Daliang et al.,2016;扬子板块,Wang Xiaolei et al.,2007;Sun Weihua et al.,2009;Xie Shiwen et al.,2009;Zhang Xiong et al.,2016

Ages sources:the Shennongjia Group,Li Huaikun et al.,2013;the Zhengjiaya Formation,Xu Daliang et al.,2016;the Yangtze Plate,Wang Xiaolei et al.,2007;Sun Weihua et al.,2009;Xie Shiwen et al.,2009;Zhang Xiong et al.,2016

普遍富集,Nb、Ta略亏损,具有弱的负Eu异常等特征(湖北地质矿产局,1990;Deng Qi et al.,2013;Hu Zhengxiang et al.,2015)。

花山群下部的洪山寺组不整合覆盖于打鼓石群之上,主体岩性为砾岩、含砾砂岩、砂岩等,总体来看自下而上粒度由粗变细,斜层理、冲刷面等沉积构造发育。砾石成分复杂,包括砂岩、硅质岩、白云岩等,磨圆度、分选度均较差,胶结物以硅质、白云质为主,充分反映其沉积过程中陆源碎屑物质供给充足,搬运距离较近,属于近物源区的快速堆积;花山群上部的六房咀组是一套以板岩为主的细碎屑沉积,主要发育水平层理,伴随有较频繁的火山活动;说明花山群整体具有“磨拉石”或“类磨拉石”沉积建造的特点。由此,花山群下部磨拉石堆积具有以下特征:① 内部发育拉斑质火山岩;② 与下伏打鼓石群呈角度不整合接触;③ 物源主要来自下伏打鼓石群;按照Xia Bangdong and Fang Zhong(1989)的磨拉石盆地分类,其构造环境应该属于拉张背景下的陆内裂谷盆地,并伴随有陆壳减薄作用。而且,根据新近的年代学研究(Li Huaikun et al.,2016),花山群下伏地层打鼓石群形成于约1230 Ma Columbia超大陆裂解背景之下,继而在约1100 Ma包括扬子北缘在内的多个大陆发育了大量的基性岩浆活动,例如:神农架地区石槽河组中约1115 Ma基性侵入体(Li Huaikun et al.,2013)、郑家垭组1103±8 Ma玄武质凝灰岩(Qiu Xiaofei et al.,2011)、非洲中南部Kalahari克拉通内部及南极洲Grunehogna地区1112～1106 Ma基性岩墙群(Hanson et al.,2006)、加拿大东部格林威尔1177±5 Ma基性岩墙/岩床(Ernst, 2007)、格陵兰地区1163±5 Ma巨型岩墙(Buchan and Ernst, 2004)等等。Qiu Xiaofei et al.(2011)认为该时期岩浆事件是扬子板块和澳大利亚板块汇聚过程的产物;Peng Songbai et al.(2012)认为1150～980 Ma弧前扩张导致扬子北缘庙湾蛇绿岩的形成,并且碰撞作用在850～830 Ma仍在引发庙湾蛇绿岩的变形和扬子北缘的变质作用;Ling Wenli et al.(2003)认为扬子板块西北缘950～895 Ma岩浆活动形成于岛弧环境。因此,结合前人在花山蛇绿混杂岩中获得的～950 Ma辉长岩年龄(Shi Yuruo et al.,2007)和约840 Ma土门英安岩年龄(Hu Zhengxiang et al.,2015),我们认为花山蛇绿混杂岩形成于Columbia超大陆裂解之后、Rodinia超大陆汇聚背景之下,与花山群中的基性岩浆活动的形成时代和形成背景完全不同。也就是说,花山群中所夹枕状玄武岩等基性火山岩、火山碎屑岩等形成于拉张背景,与其东部的“蛇绿混杂岩”中的岩浆岩非同期的岩浆活动,形成背景也有拉张和挤压的截然区别。正如前述,花山群更可能是在900～815 Ma之间的某个节点(很可能是820 Ma)

挤压-伸展转换完成之后开始沉积的。

在南华裂谷盆地发现的一系列不连续的楔状沉积体不整合于约 825 Ma 花岗质岩石之上，其沉积时代起始于 820 Ma 左右（Wang Jian and Li Zhengxiang，2003），由此推测，约 820 Ma 发生的大规模的地壳抬升和顶侵作用在华南地区是普遍存在的，也说明在约 820 Ma 前后可能经历了陆-陆碰撞造山旋回结束——伸展裂解的转换，这一转换机制的驱动力则很可能来自于地幔柱作用，这一点可以得到扬子周缘大量约 820 Ma 酸性—基性岩浆活动的佐证。

5.5　花山群与新元古代超大陆事件的关系

扬子板块北缘、西缘及南缘普遍存在约 820 Ma 岩浆活动，例如约 820 Ma 的铁船山拉斑玄武岩（Ling Wenli et al.，2003）、约 800 Ma 的康滇地区双峰式玄武岩（Li Xianhua et al.，2002）、约 827 Ma 的广丰碱性玄武岩（Li Wuxian et al.，2008）、约 815 Ma 黄陵侵入体中辉长岩、闪长岩（Wu Hui et al.，2016）等。新元古代晚期裂解的地质记录也大量存在于我国柴达木、塔里木和华北等板块周缘：柴达木北缘 850～820 Ma 基性岩墙及火山活动（Lu Songnian et al.，2008；Xu Xin et al.，2016）、塔里木板块北缘 825～800 Ma 的超镁铁质—镁铁质-碳酸岩岩浆侵入事件（Zhang Chuanlin et al.，2011，2012）以及～827 Ma 华北板块西缘金川辉长岩（Li Xianhua et al.，2004）等。综合中国几个克拉通上的相关资料（Wang Jian，2000；Wang Jian et al.，2003；Li Zhengxiang et al.，2008；Zhang Qirui et al.，2008；Zhao Junhong et al.，2011）表明 Rodinia 超大陆裂解启动时间为 820～800 Ma。

Kampumzu et al.（2000）提出岩浆活动如果以裂谷大陆拉斑玄武岩和酸性岩浆共生为起始则多与热点作用有关；基于 828～820 Ma 镁铁质—超镁铁质侵入体及花岗质岩体，Li Xianhua et al（1999，2003）提出约 825 Ma 扬子板块存在地幔柱，该时段岩浆活动形成于地幔柱作用导致的地壳重熔背景之下，Wang Xuance et al.（2007）研究认为益阳科马提质玄武岩（823±6 Ma）的岩浆温度可能达到 1500 度以上。而且扬子周缘地区 825～820 Ma 的基性—超基性岩浆活动可以与澳大利亚 Gairdner 岩墙群相对比（Li Xianhua et al.，2003），600 Ma 之前的新元古代裂谷盆地可与澳大利亚东南部的 Adelaide 裂谷系相对比（Wingate et al.，1998；Wang Jian and Li Zhengxiang，2003）；反映约 820 Ma 地幔柱作用广泛存在并直接导致了 Rodinia 超大陆的裂解。

Wang Jian and Li Zhengxiang（2003）认为 Rodinia 超大陆裂解过程中，早期裂谷作用在扬子板块表现为约 820 Ma 的石桥铺组（最新年龄 828.8±9.6 Ma，Luo Lai et al.，2016）和 800 Ma 左右的虹赤村组沉积。近年来，扬子周缘一系列同期沉积地层获得了精确的年代学约束：约 814 Ma 下江群甲路组（Gao Linzhi et al.，2010）、约 824 Ma 河上镇群骆家门组（Zhang Heng et al.，2015）、～800 Ma 板溪群张家湾组（Gao Linzhi et al.，2011）等，由此推测花山群六房咀组与该时期地层同属 Rodinia 超大陆第一期裂解（820～800 Ma，Wang Jian and Li Zhengxiang，2003）在扬子周缘的响应。

综上所述，扬子北缘与 Rodinia 超大陆初始裂解相对应的裂解事件始于约 820 Ma，扬子板块北缘裂解与东南缘裂解至少在时限上（约 820 Ma，Wang Jian and Li Zhengxiang，2003；Zhang Qirui，2008）是一致的。

6　结论

（1）来自花山群六房咀组和南华系莲沱组的三件碎屑岩样品的年龄峰值与扬子克拉通碎屑锆石年龄谱统计峰值基本一致。花山群六房咀组碎屑岩具有相对一致的年龄谱特征，存在三个峰值：～900 Ma、～2050 Ma 和～2650 Ma，最明显峰值为～2650 Ma；花山群上覆莲沱组碎屑岩年龄谱存在三个峰值：～900 Ma、～2050 Ma 和～2500 Ma，最明显峰值为～2050 Ma，反映二者碎屑源区存在较大差异；花山群六房咀组熔结凝灰岩锆石年龄为 814.7±7.3 Ma，最年轻碎屑锆石峰值为～900 Ma，结合花山群中～820 Ma 基性火山岩年龄，说明花山群形成时代应该在 820～815 Ma。

（2）花山群枕状玄武岩与其中的基性火山碎屑岩为同期火山活动产物，形成于深部扩张环境，与花山"蛇绿混杂岩"带内的岩浆岩不是同期同构造背景的产物。

（3）花山群形成于 Rodinia 超大陆裂解背景之下，扬子北缘的裂解时代与东南缘一致，与超级地幔柱活动有关。

致谢：锆石 U-Pb 同位素测年得到北京离子探针中心刘敦一研究员、张玉海研究员和宋彪研究员等的大力支持和帮助，任纪舜院士和陆松年研究员等对我们的研究工作给予了长期的指导和帮助，锆

石分选等样品前处理工作由河北省廊坊市宇能岩石矿物分选技术服务有限公司王建华高工完成，薄片鉴定工作由河北省廊坊区域地质矿产调查所实验室完成，同位素测年实验过程中还得到任云伟、张家辉、孙凯、崔玉荣等的帮助，野外调研期间得到湖北省国土资源厅曹微、神农架国家地质公园管理局王志先、李晓池和钟权等支持和帮助，在此一并致以诚挚的感谢。

注 释

❶ 湖北省地质矿产局.1982. 1∶20 万随县幅区域地质调查报告.

❷ 湖北省地质矿产局.1982. 1∶20 万宜城幅区域地质调查报告.

References

Anderson T. 2002. Correction of common lead in U-Pb analyses that do not report ^{204}Pb. Chemical Geology, 192(1/2): 59～79.

Black L P, Kamo S L, Allen C M, Aleinikoff, Davis D W, Korsch R J, Foudoulis C A. 2003. New zirconstandard for Phanerozoic U-Pb geochronology. Chemical Geology, 200(1-2): 155～170.

Buchan K L, Ernst R E. 2004. Diabase dyke swarms and related units in Canada and adjacent regions. In: Geological Survey of Canada, "A" Aeries Map. 2022A (scale 1∶5000000).

Compston W, Williams I S, Meyer C. 1984. U-Pb geochronology of zircons from lunar breccia 73217 using a sensitive high mass-resolution ion microprobe. Journal of Geophysical Research, 14(2): 525～534.

Compston W, Williams I S, Krischvink J L, Zhang Z, Ma G G. 1992. Zircon U-Pb ages for the Early Cambrian time-scale. Journal of the Geological Society, 149(2): 171～184.

Deng Qi, Wang Jian, Wang Zhengjiang, Wang Xuance, Qiu Yansheng, Yang Qingxiong, Du Qiuding, Cui Zhuang, Zhou Xiaolin. 2013. Continental flood basalts of the Huashan Group, northern margin of the Yangtze block-implications for the breakup of Rodinia. International Geology Review, 55(15): 1865～1884.

Dong Yunpeng, Zhang Guowei, Liu Xiaoming, Lai Shaocong. 1998. Disintegration of the Huashan Group in the Dahong Mountain area, northern Hubei. Regional Geology of Chin, 17(4): 371～376 (in Chinese with English abstract).

Dong Yunpeng, Zhang Guowei, Lai Shaocong, Zhou Dingwu Zhu Bingquan. 1999. An ophiolitic tectonic melange first discovered in Huashan area, south margin of Qinling Orogenic Belt, and its tectonic implications. Science in China (Series D), 29(3): 222～231 (in Chinese).

Dong Yunpeng, Zhang Guowei, Yao Anping, Zhao Xia. 2003. Deformation and evolution of the Sanligang-Sanyang tectonic mélange belt along the west sector of Xiangfan-Guangji fault. Chinese Journal of Geology, 38(4): 425～436 (in Chinese with English abstract).

Ernst R E. 2007. Large igneous provinces in Canada through time and their metallogenic potential. In: Goodfellow W D, ed. Mineral Deposits of Canada: A Synthesis of Major Deposit Types, District Metallogeny, the Evolution of Geological Provinces and Exploration Methods. Geological Association of Canada, Mineral Deposits Division, Special Publication, 5: 929～937.

Evans D A D, Mitchell R N. 2011. Assembly and breakup of the core of Paleoproterozoic-Mesoproterozoic supercontinent Nuna. Geology, 39(5): 443～446.

Garnier V, Ohnenstetter D, Giuliani G, Fallick A E, Phan T T, Hoangquang V, Pham V L, Schwarz D. 2005. Basalt petrology, zircon ages and sapphire genesis from Dak Nong, southern Vietnam. Mineralogical Magazine, 69(1): 21～38.

Gao Linzhi, Dai Chuangu, Liu Yanxue, Wang Min, Wang Xuehua, Chen Jianshu, Ding Xiaozhong. 2010. Zircon SHRIMP U-Pb dating of the tuffaceous bed of Xiajiang Group in Guizhou Province and its stratigraphic implication. Geology In China, 37(4): 1071～1080 (in Chinese with English abstract).

Gao Linzhi, Chen Jun, Ding Xiaozhong, Liu Yaorong, Zhang Chuanheng, Zhang Heng, Liu Yanxue, Pang Weihua, Zhang Yuhai. 2011. Zircon SHRIMP U-Pb dating of the tuff bend of Lengjiaxi and Banxi groups, northern Hunan: constraints on the Wuling Movement. Geological Bulletin of China, 30(7): 1001～1008 (in Chinese with English abstract).

Geng Jianzhen, Zhang Jian, Li Huaikun, Li Huimin, Zhang Yongqing, Hao Shuang. 2012. Ten-micron-sized zircon U-Pb dating using LA-MC-ICP-MS. Acta Geoscientica Sinica, 33(6): 877～884 (in Chinese with English abstract).

Hanson R E, Harmer R E, Blenkinsop T G, Bullen D S, Dalziel I W D, Gose W A, Hall R P, Kampunzu A B, Key R M, Mukwakwami J, Munyanyiwa H, Pancake JA, Seidel E K, Ward S E. 2006. Mesoproterozoic intraplate magmatismin the Kalahari Craton: A review. Journal of African Earth Sciences, 46(1-2): 141～167.

Hoffman P F. 2007. Speculations on Laurentia's first gigayear (2.0 to 1.0 Ga). Learning & Memory, 14(3): 117～125.

Hou Kejun, Li Yanhe, Tian Yourong. 2009. In situ U-Pb zircon dating using laser ablation-multi ion counting-ICP-MS. Mineral Deposits, 28(4): 481～492 (in Chinese with English abstract).

Hu Zhengxiang, Chen Chao, Mao Xinwu, Deng Qianzhong, Yang Jinxiang, Li Linjing, Kong Lingyao. 2015. Documentation of Jinningianisland-arc volanic rocks and accretionary complexes in the Dahongshan region, northern Hubei and its tectonic significance. Resources Environment & Engineering, 29(6): 757～766 (in Chinese with English abstract).

Hubei Geological and Mineral Resources Bureau. 1990. Regional Geology of Hubei Province. Beijing: Geological Publishing House, 1～705 (in Chinese with English abstract).

Jackson S E, Pearson N J, Griffin W L. 2004. The application of laser ablation-inductively coupled plasma-mass spectrometry to in situ U-Pb zircon geochronology. Chemical Geology, 211: 47

～69.

Kampunzu A B, Tembo F, Matheis G, Kapenda D, Huntsman P. 2000. Geochemistry and tectonic setting of mafic igneous units in the Neoproterozoic Katangan Basin, Central Africa: Implications for Rodinia break-up. Gondwana Research, 3(2): 125～153.

Larson R L. 1991. Geological consequences of superplumes. Geology, 19(10): 963～966.

Li Huaikun, Geng Jianzhen, Hao Shuang, Zhang Yongqing, Li Huimin. 2009. Study on testing U-Pb istopic age of zircon with LA-MC-ICPMS. Mineral Sinica, 28: 76～77 (in Chinese).

Li Huaikun, Zhang Chuanlin, Xiang Zhenqun, Lu Songnian, Zhang Jian, Geng Jianzhen, Qu Lesheng, Wang Zhixian. 2013. Zircon and baddeleyite U-Pb geochronology of the Shennongjia Group in the Yangtze Craton and its tectonic significance. Acta Petrological Sinica, 29(2): 673～697 (in Chinese with English abstract).

Li Huaikun, Tian Hui, Zhou Hongying, Zhang Jian, Liu Huan, Geng Jianzhen, Ye Lijuan, Xiang Zhenqun, Qu Lesheng. 2016. Correlation between the Dagushi Group in the Dahongshanarea and the Shennongjia Group in the Shennongjia area on the northern margin of the Yangtze Craton: Constraints from zircon U-Pb ages and Lu-Hf isotopic systematic. Earth Science Frontiers, 23(6): 186～201 (in Chinese with English abstract).

Li Jinyi. 2002. Doubt about the age of the original Liantuo Formation in the Dahongshan area, Hubei Province, Central China. Geological Bulletin of China, 21(8): 579～583 (in Chinese with English abstract).

Li Sanzhong, Zhang Guowei, Li Yalin, Lai Shaocong, Li Zonghui. 2002. Deformation and orogeny of the Mian-Luesuture zone in the Qinling orogenic belt. Acta Geologica Sinica, 76(4): 469～483 (in Chinese with English abstract).

Li Wuxian, Li Xianhua, Li Zhengxiang. 2008. Middle Neoproterozoic syn-rifting volcanic rocks in Guangfeng, South China: Petrogenesis and tectonic significance. Geological Magazine, 145(4): 475～489.

Li Xianhua. 1999. U-Pb zircon ages of granites from the southern margin of the Yangtze Block: timing of Neoproterozoic Jinning: Orogeny in SE China and implications for Rodinia assembly. Precambrian Research, 97(1): 43～57.

Li Xianhua, Zhou Guoqing, Zhao Jianxin. 1994. SHRIMPion microprobe zircon U-Pb age of the NE Jiangxi ophiolite and its tectonic implications. Geochimica, 23(2): 125～131 (in Chinese with English abstract).

Li Xianhua, Li Zhengxiang, Zhou Hanwen, Liu Ying, Kinny P D. 2002. U-Pb zircon geochronology, geochemistry and Nd isotopic study of Neoproterozoic bimodal volcanic rocks in the Kangdian Rift of South China: Implications for the initial rifting of Rodinia. Precambrian Research, 113(1-2): 135～154.

Li Xianhua, Li Zhengxiang, Ge Wenchun, Zhou Hanwen, Li Wuxian, Liu Ying, Michael T D. 2003. Neoproterozoic granitoids in South China: crustal melting above a mantle plume at ca. 825 Ma? Precambrian Research, 122(1-4): 45～83.

Li Xianhua, Su Li, Song Biao, Liu Dunyi. 2004. SHRIMP U-Pb zircon age of the Jinchuan ultramafic intrusion and its geological significance. Science Bulletin, 49(4): 420～422.

Li Xianhua, Li Wuxian, Li Zhengxiang, Liu Ying. 2008a. 850～790 Ma bimodal volcanic and intrusive rocks in northern Zhejiang, South China: A major episode of continental rift magmatism during the breakup of Rodinia. Lithos, 102(1-2): 341～357.

Li Xianhua, Wang Xuance, Li Wuxian, Li Zhengxiang. 2008b. Petrogenesis and tectonic significance of Neoproterozoic basaltic rocks in South China: From orogenesis to intracontinental rifting. Geochimica, 37 (4): 382～398.

Li Zhengxiang. 1999. 830～820 Ma mafic to felsic igneous activity in South China and the breakup of Rodinia. Gondwana Research, 2(4): 591～591.

Li Zhengxiang, Zhang Linghua, Powell C M A. 1995. South China in Rodinia: Part of the missing link between Australia East Antarctica and Laurentia? Geology, 23(5): 407～410.

Li Zhengxiang, Li Xianhua, Kinny P D, Wang Jian. 1999. The breakup of Rodinia: did it start with a mantle plume beneath South China? Earth & Planetary Science Letters, 173(3): 171～181.

Li Zhengxiang, Li Xianhua, Kinny P D, Wang Jian, Zhang Sheng, Zhou Hui. 2003. Geochronology of Neoproterozoic syn-rift magmatism in the Yangtze Craton, South China and correlations with other continents: evidence for a mantle superplume that broke up Rodinia. Precambrian Research, 122 (1-4): 85～109.

Li Zhengxiang, Bogdanova S V, Collins A S, Davidson A, Waele B D, Ernst R E, Fitzsimons I C W, Fuck R A, Gladkochub D P, Jacobs J, Karlstrom K E, Lu S N, Natapov L M, Pease V, Pisarevsky S A, Thrane K, Vernikovsky V. 2008. Assembly, configuration, and break-up history of Rodinia: A synthesis. Precambrian Research, 160(1-2): 179～210.

Li Zuochen, Pei Xianzhi, Li Ruibao, Pei Lei, Liu Chengjun, Chen Youxin, Xu Tong, Yang Jie, Wei Bo. 2015. U-Pb zircon geochronology and geochemistry of the Neoproterozoic Liujiaping Group volcanics in the northwest margin of the Yangtze block: Implications for the breakup of the Rodinia supercontinent. Acta Geologica Sinica, 89(4): 1213～1225.

Liermann H P, Isachsen C, Altenberger U, Oberhansli R. 2002. Behavior of zircon during high-pressure, low-temperature metamorphism: Case study from the internal unit of the Sesia zone (western Italian Alps). Acoustics Speech & Signal Processing Newsletter IEEE, 14(1): 61～71.

Lin Guangchun, Li Xianhua, Li Wuxian. 2007. SHRIMP U-Pb zircon age, geochemistry and Nd-Hf isotope of Neoproterozoic mafic dyke swarms in western Sichuan: Petrogenesis and tectonic significance. Science in China, 50(1): 1～16.

Ling Wenli, Gao Shan, Ouyang Jianping, Zhang Benren, Li Huimin. 2002. Age and tectonic background of Xixiang Group: isotopic chronology and geochenmical constraints. Science in China, 32(2): 101～112 (in Chinese).

Ling Wenli, Gao Shan, Zhang Benren, Li Huimin, Liu Ying, Cheng Jianping. 2003. Neoproterozoic tectonic evolution of the northwestern Yangtze craton, South China: implications for amalgamation and break-up of the Rodinia Supercontinent. Precambrian Research, 122(1－4): 111～140.

Liu Yongsheng, Hu Zhaochu, Zong Keqing, Gao Changgui, Gao Shan, Xu Juan, Chen Haihong. 2010. Reappraisement and refinement of zircon U-Pb isotope and trace element analyses by LA-ICP-MS. Chinese Science Bulletin, 55(15): 1535～1546.

Lu Songnian. 2001. From Rodinia to Gondwanaland supercontinents——Thing about problems of researching Neoproterozoic supercontinents. Earth Science Frontiers, 8 (4): 441～448 (in Chinese with English abstract).

Lu Songnian, Zhao Guochun, Wang Huichu, Hao Guojie. 2008. Precambrian metamorphic basement and sedimentary cover of the North China Craton: A review. Precambrian Research, 160 (1-2): 77～93.

Lu Songnian, Xiang Zhenqun, Li Huaikun, Wang Huichu, Chu Hang. 2012. Response of the North China Craton to Rodinia supercontinental events-GOSEN Joining Hypothesis. Acta Geologica Sinica, 86(9): 1396～1406 (in Chinese with English abstract).

Luo Lai, He Liang, Sun Haiqing, Huang Jianzhong. 2016. Zicon SHRIMP U-Pb age of Gaojian Group in the Southeastern margin of Yangtze Craton. Geology and Mineral Resources of South China, 32 (1): 15 ～ 20 (in Chinese with English abstract).

Ludwig K R. 2003a. User's manual for Isoplot/Ex v., version 3. 00: A Geochronological Toolkit for Microsoft Excel. Berkeley Geochronology Center Special Publication, 4(1): 1～70.

Ludwig K R. 2003b. User's manual for Isoplot/Ex, version 3. 70. A Geochronological Toolkit for Microsoft Excel. Berkeley Geochronology Center Special Publication, 4: 1～76.

Meert J G. 2012. What's in a name? The Columbia (Paleopangaea/ Nuna) supercontinent. Gondwana Research, 21 (4): 987 ～993.

Nasdala L, Hofmeister W, Norberg N, Martinson J M, Corfu F, Dorr W, Kamo S L, Kennedy A K, Kronz A, Reiners P W, Frei D, Kosler J, Wan Y S, Gotze J, Hager T, Kroner A, Valley J W. 2008. Zircon M257-A homogeneous natural reference material for the ion microprobe U-Pb analysis of zircon. Geostandards and Geoanalytical Research, 32(3): 247 ～265.

Peng Songbai, Kusky T M, Jiang Xingfu, Deng Hao. 2012. Geology, geochemistry, and geochronology of the Miaowan ophiolite, Yangtze craton: Implications for South China's amalgamation history with the Rodinian supercontinent. Gondwana Research, 21(2－3): 577～594.

Qiu Xiaofei, Ling Wenling, Liu Xiaoming, Kusky T, Berkana W, Zhang Yinghua, Gao Yongjuan, Lu Shansong, Kuang Hua, Liu Chengxin. 2011. Recognition of Grenvillian volcanic suite in the Shennongjia region and its tectonic significance for the South China Craton. Precambrian Research, 191(3-4): 101 ～119.

Rogers J W, Santosh M. 2002. Configuration of Columbia, a Mesoproterozoic Supercontinent. Gondwana Research, 5(1): 5 ～22.

Santosh M, Maruyama S, Yamamoto S. 2009. The making and breaking of supercontinents: Some speculations based on superplumes, super downwelling and the role of tectosphere. Gondwana Research, 15(3-4): 324～341.

Shi Yuruo, Liu Dunyi, Zhang Zongqing, Miao Laicheng, Zhang Fuqin, Xue Hongmei. 2007. SHRIMP zircon U-Pb dating of gabbro and granite from the Huashan ophiolite, Qinling orogenic belt, China: Neoproterozoic suture on the northern margin of the Yangtze Craton. Acta Geological Sinica. 81(2): 239～243.

Song Biao, Zhang Yuhai, Wan Yusheng. 2002. Mount making and procedure of the SHRIMP dating. Geological Review, 48 (supplementary): 26～30 (in Chinese with English abstract).

Song Fang, Niu Zhijun, He Yaoyan, Yang Wenqiang. 2016. U-Pb age of detrital zircon and its restriction of provenance &paleogeographic characteristics of early Nanhua period in Middle Yangtze. Acta Geologica Sinica, 90(10): 2661～2680 (in Chinese with English abstract).

Sun Weihua, Zhou Meifu, Gao Jianfeng, Yang Yueheng, Zhao Xinfu, Zhao Junhong. 2009. Detrital zircon U-Pb geochronological and Lu-Hf isotopic constraints on the Precambrian magmatic and crustal evolution of the western Yangtze Block, SW China. Precambrian Research, 172(1-2): 99～126.

Wang Jian. 2000. NeoproterozoicRifting History of South China: Significance to Rodinia Breakup. Beijing: Geological Publishing House, 1～146 (in Chinese with English abstract).

Wang Jian, Li Zhengxiang. 2003. History of Neoproterozoic rift basins in South China: implications for Rodinia break-up. Precambrian Research, 122(1－4): 141～158.

Wang Jian, Li Xianhua, Duan Taizhong, Liu Dunyi, Song Biao, Li Zhongxiong, Gao Yonghua. 2003. Zircon SHRIMP U-Pb dating for the Cangshuipu volcanic rocks and its implications for the lower boundary age of the Nanhua strata in South China. Chinese Science Bulletin, 48(16): 1663～1669.

Wang Lijuan, Yu Jinhai, Griffin W L, O'Reilly S Y. 2011. Early crustal evolution in the western Yangtze Block: Evidence from U-Pb and Lu-Hf isotopes on detrital zircons from sedimentary rocks. Precambrian Research, 222－223: 368～385.

Wang Tao, Zhang Zongqing, Wang Xiaoxia, Wang Yanbin, Zhang Chengli. 2005. Neoproterzoic collisional deformation in the core of the Qinling orogen and its age: constrained by zircon SHRIMP dating of strongly deformed syn-collisional granites and weakly deformed granite veins. Acta Geologica Sinica, 79 (2): 220～231 (in Chinese with English abstract).

Wang Wei, Zhou Meifu, Yan Danping, Li Jianwei. 2012. Depositional age, provenance, and tectonic setting of the Neoproterozoic Sibao Group, southeastern Yangtze Block, South China. Precambrian Research, 192(1): 107～124.

Wang Xiaolei, Jiang Shaoyong, Dai Baozhang, Griffin W L, Dai Mengning, Yang Yueheng. 1982. Age, geochemistry and tectonic setting of the Neoproterozoic (ca 830 Ma) gabbros on the southern margin of the North China Craton. Economic Geology, 77(1): 273～293.

Wang Xiaolei, Zhou Jincheng, Qiu Jiansheng, Gao Jianfeng. 2004. Geochemistry of the Meso-to Neoproterozoic basic-acid rocks from Hunan Province, South China: implications for the evolution of the western Jiangnan orogen. Precambrian Research, 135(1): 79～103.

Wang Xiaolei, Zhou Jincheng, Qiu Jiansheng, Zhang Wenlan, Liu Xiaoming, Zhang Guilin. 2006. LA-ICP-MS U-Pb zircon geochronology of the Neoproterozoic igneous rocks from Northern Guangxi, South China: Implications for tectonic evolution. Precambrian Research, 145(1-2): 111～130.

Wang Xiaolei, Zhou Jincheng, Griffin W L, Wang Rucheng, Qiu Jiansheng, O'Reilly S Y, Xu Xisheng, Liu Xiaoming, Zhang Guilin. 2007. Detrital zircon geochronology of Precambrian basement sequences in the Jiangnan orogen: Dating the assembly of the Yangtze and Cathaysia Blocks. Precambrian Research, 159(1-2): 117～131.

Wang Xiaolei, Shu Liangshu, Xing Guangfu, Zhou Jincheng, Tang Ming, Shu Xujie, Qi Liang, Hu Yanhua. 2014a. Post-orogenic extension in the eastern part of the Jiangnan orogen: Evidence from ca, 800～760 Ma volcanic rocks. Precambrian Research, 222－223: 404～423.

Wang Xiaolei, Zhou Jincheng, Griffin W L, Zhao Guochun, Yu Jinhai, Qiu Jiansheng, Zhang Yanjie, Xing Guangfu. 2014b. Geochemical zonation across a Neoproterozoic orogenic belt: Isotopic evidence from granitoids and metasedimentary rocks of the Jiangnan orogen, China. Precambrian Research, 242(2): 154～171.

Wang Xuance, Li Xianhua, Li Wuxian, Li Zhengxiang. Ca. 2007. 825 Ma komatiitic basalts in South China: First evidence for ＞1500 degrees C mantle melts by a Rodinian mantle plume. Geology, 35(12): 1103～1106.

Williams I S. 1998. U-Th-Pb geochronology by ion microprobe. In: McKibben M A, Shanks W C, Ridley W I eds. Applications of Microanalytical Techniques to Understanding Mineralizing Process. Review of Economic Geology, 7(1): 1～35.

Wingate M T D, Campbell I H, Compston W, Gibson G M. 1998. Ion microprobe U-Pb ages for Neoproterozoic basaltic magmatism in south-central Australia and implications for the breakup of Rodinia. Precambrian Research, 87(3): 135～159.

Wu Hui, Zhang Yinghua, Ling Wenli, Bai Xiao, Ma Qian, Berkana W, Cheng Jianping, Peng Lianhong. 2016. Recognition of mantle input and its tectonic implication for the nature of ～815 Ma magmatism in the Yangtze continental interior, South China. Precambrian Research, 279: 17～36.

Xia Bangdong, Fang Zhong. 1989. Molasse and global tectonics. Experimental Petroleum Geology, 11(4): 314～319 (in Chinese with English abstract).

Xie Jifeng, Zhang Benren. 2000. Geochemistry of the Anzishan Ophiolitic Complex in the Mian-Lue belt of Qinling orogen. Acta Geologica Sinica, 74(1): 39～50 (in Chinese with English abstract).

Xie Shiwen, Gao shan, Liu Xiaoming, Gao Risheng. 2009. U-Pbages and Hf isotope of detrital zircons of Nanhua sedimentary rocks from the Yangtze Gorges: Implications for genesis of Neoproterozoic magmatism in South China. Earth Science-Journal of China University of Geosciences, 34(1): 117～126 (in Chinese with English abstract).

Xu Daliang, Liu Hao, Wei Yunxu, Peng Lianhong, Deng Xin. 2016. Detrital zircon U-Pb dating of Zhengjiaya Formation from the Shennongjiaarea in the northern Yangtze block and its tectonic implications. Acta Geologica Sinica, 90(10): 2648～2660 (in Chinese with English abstract).

Xu Xin, Song Shuguang, Allen M B, Ernst R E, Niu Yaoling, Su Li. 2016. An 850-820 Ma LIP dismembered during breakup of the Rodinia supercontinent and destroyed by Early Paleozoic continental subduction in the northern Tibetan Plateau, NW China. Precambrian Research, 282: 52～73.

Xu Zhiqin, Li Yuan, Liang Fenghua, Pei Xianzhi. 2015. A connection between of the Paleo-Tethyssutrure zone in the Qinling-Dabie-Sulu orogenic belt. Acta Geologica Sinica, 89 (4): 671～680 (in Chinese with English abstract).

Yan Quanren, Wang Zongqi, Hanson A D, Druschke P A, Yan Zhen, Liu Dunyi, Jian Ping, Song Biao, Wang Tao, Jiang Chunfa. 2003. SHRIMP age and geochemistry of the Bikou volcanic terrane: Implications for Neoproterozoic tectonics on the northern margin of the Yangtze Craton. Acta Geologica Sinica, 77(4): 479～490.

Zhang Chuanlin, Yang Dongsheng, Wang Hongyan, Takahashi Y, Ye Haimin. 2011. Neoproterozoic mafic-ultramafic layered intrusion in Quruqtagh of northeastern Tarim Block, NW China: Two phases of mafic igneous activity with different mantle sources. Gondwana Research, 19(1): 177～190.

Zhang Chuanlin, Zou Haibo, Wang Hongyan, Li Huaikun, Ye Haimin. 2012. Multiple phases of the Neoproterozoic igneous activity in Quruqtagh of the northeastern Tarim Block, NW China: Interaction between plate subduction and mantle plume?. Precambrian Research, 222～223: 488～502.

Zhang Heng, Gao Linzhi, Li Tingdong, Geng Shufang, Liu Yanxue, Ding Xiaozhong, Shi Zhigang. 2015. SHRIMP zircon U-Pb dating of the Luojiamen Formation in western Zhejiang Province and its geological implications. Geological Bulletin of China, 34 (2-3): 447～455 (in Chinese with English abstract).

Zhang Qirui, Song Biao, Li Xianhua, Feng Lianjun, Huang Jing, Song Biao. 2008. A new age constraint on the onset of the Neoproterozoic glaciations in the Yangtze Platform, South China. Journal of Geology, 116(4): 423~429.

Zhang Xiong, Zeng Zuoxun, Pan Lili, Zeng Zhihui, Peng Lianhong, Xu Daliang, Wei Yunxu, Liu Hao, Deng Xin. 2016. Recognition of the sedimentation age of a series of purple-red colored glutenite sedimentary rocks in Dahong Mountain area, northern Hubei Province: Detrital zircon U-Pb geochronology and its geological significance. Geological Bulletin of China, 35 (7): 1069~1080 (in Chinese with English abstract).

Zhang Zhongying, Zhao Yinsheng. 1989. Microfossils from the Dagushi Group in the Dahongshan area, northern Hubei Province. Geological Review, 35(1): 84~89 (in Chinese with English abstract).

Zhang Zongqing, Zhang Guowei, Tang Suohan, Wang Jinhui. 2001. On the age of metamorphic rocks of the Yudongzi Group and the Archean crystalline basement of the Qinling orogen. Acta Geologica Sinica, 75 (2): 198 ~ 204 (in Chinese with English abstract).

Zhao Guochun. 2012. Precambrian geology of China: An introduction. Precambrian Research, 222－223: 13~54.

Zhao Guochun, Cawood P A, Wilde S A, Sun Min. 2002. Review of global 2.1~1.8 Ga orogens: implications for a Pre-Rodinia supercontinent. Earth-Science Reviews, 59(1): 125~162.

Zhao Junhong, Zhou Meifu. 2007a. Geochemistry of Neoproterozoic mafic intrusions in the Panzhihua district (Sichuan Province, SW China): Implications for subduction-related metasomatism in the upper mantle. Precambrian Research, 152(1): 27~47.

Zhao Junhong, Zhou Meifu. 2007b. Neoproterozoic adakitic plutons and arc magmatism along the western margin of the Yangtze Block, South China. Journal of Geology, 115(6): 675~689.

Zhao Junhong, Zhou Meifu. 2008. Neoproterozoic adakitic plutons in the northern margin of the Yangtze Block, China: Partial melting of a thickened lower crust and implications for secular crustal evolution. Lithos, 104(1): 231~248.

Zhao Junhong, Zhou Meifu. 2009a. Melting of newly formed mafic crust for the formation of Neoproterozoic I-type granite in the Hannan region, South China. Journal of Geology, 117(1): 54~70.

Zhao Junhong, Zhou Meifu. 2009b. Secular evolution of the Neoproterozoic lithospheric mantle underneath the northern margin of the Yangtze Block, South China. Lithos, 107(3): 152~168.

Zhao Junhong, Zhou Meifu, Yan Danping, Zheng Jianping, Li Jianwei. 2011. Reappraisal of the ages of Neoproterozoic strata in South China: No connection with the Grenvillian orogeny. Geology, 39(4): 299~302.

Zheng Yongfei, Zhang Shaobing. 2007. Formation and evolution of Precambrian continental crust. Chinese Science Bulletin, 52 (1): 1~10.

Zheng Yongfei, Zhang Shaobing, Zhao Zifu, Wu Yuanbao, Li Xianhua, Li Zhengxiang, Wu Fuyuan. 2007. Contrasting zircon Hf and O isotopes in the two episodes of Neoproterozoic granitoids in South China: Implications for growth and reworking of continental crust. Lithos, 96(1-2): 127~150.

Zhou Jincheng, Wang Xiaolei, Qiu Jiansheng, Gao Jianfeng. 2004. Geochemistry of Meso-and Neoproterozoic mafic-ultramafic rocks from northern Guangxi, China: Arc or plume magmatism? Geochemical Journal, 38(2): 139~152.

Zhou Meifu, Michael Lesher C. 2002. Neoproterozoic arc-related mafic intrusions along the northern margin of South China: Implications for the accretion of Rodinia. Journal of Geology, 110(5): 611~618.

Zhou Meifu, Yan Danping, Kennedy A K, Li Yunqian, Ding Jun. 2002. SHRIMP U-Pb zircon geochronological and geochemical evidence for Neoproterozoic arc-magmatism along the western margin of the Yangtze Block, South China. Earth & Planetary Science Letters, 196(1-2): 51~67.

Zhou Meifu, Ma Yuxiao, Yan Danping, Xia Xiaoping, Zhao Junhong, Sun Min. 2006. The Yanbian Terrane (Southern Sichuan Province, SW China): A Neoproterozoic arc assemblage in the western margin of the Yangtze Block. Precambrian Research, 144(1-2): 19~38.

Zhu Weiguang, Zhong Hong, Deng Hailin, Wilson A H, Qin Yufen. 2006. SHRIMP zircon U-Pb age, geochemistry, and Nd-Sr isotopes of the Gaojiacun mafic-ultramafic intrusive complex, Southwest China. International Geology Review, (7): 650~668.

参 考 文 献

董云鹏，张国伟，柳小明，赖绍聪. 1998. 鄂北大洪山地区“花山群”的解体. 地质通报，17(4): 371~376.

董云鹏，张国伟，赖绍聪，周鼎武，朱炳泉. 1999. 随州花山蛇绿构造混杂岩的厘定及其大地构造意义. 中国科学，29(3): 222~231.

董云鹏，张国伟，姚安平，赵霞. 2003. 襄樊-广济断裂西段三里岗-三阳构造混杂岩带构造变形与演化. 地质科学，38(4): 425~436.

高林志，戴传固，刘燕学，王敏，王雪华，陈建书，丁效忠. 2010. 黔东地区下江群凝灰岩锆石 SHRIMP U-Pb 年龄及其地层意义. 中国地质，37(4):1071~1080.

高林志，陈峻，丁孝忠，刘耀荣，张传恒，张恒，刘燕学，庞维华，张玉海. 2011. 湘东北岳阳地区冷家溪群和板溪群凝灰岩 SHRIMP 锆石 U-Pb 年龄——对武陵运动的制约. 地质通报，30(7): 1001~1008.

耿建珍，张健，李怀坤，李惠民，张永清，郝爽. 2012. 10μm 尺度锆石 U-Pb 年龄的 LA-MC-ICP-MS 测定. 地球学报，33(6): 877~884.

侯可军，李延河，田有荣. 2009. LA-MC-ICP-MS 锆石微区原位 U-Pb 定年技术. 矿床地质，28(4): 481~492.

胡正祥，陈超，毛新武，邓乾忠，杨金香，李琳静，孔令耀. 2015. 鄂北大洪山晋宁期岛弧火山岩和增生杂岩的厘定及地质意义. 资源环境与工程，29(6): 757~766.

湖北省地质矿产局. 1990. 湖北省区域地质志. 北京:地质出版社, 1～705.
李怀坤, 耿建珍, 郝爽, 张永清, 李惠民. 2009. 用激光烧蚀多接收器等离子体质谱仪(LA-MC-ICPMS)测定锆石 U-Pb 同位素年龄的研究. 矿物学报, 28(增刊): 26～77.
李怀坤, 张传林, 相振群, 陆松年, 张健, 耿建珍, 瞿乐生, 王志先. 2013. 扬子克拉通神农架群锆石和斜锆石 U-Pb 年代学及其构造意义. 岩石学报, 29(2): 673～697.
李怀坤, 田辉, 周红英, 张健, 刘欢, 耿建珍, 叶丽娟, 相振群, 瞿乐生. 2016. 扬子克拉通北缘大洪山地区打鼓石群与神农架地区神农架群的对比:锆石 SHRIMP U-Pb 年龄及 Hf 同位素证据, 地学前缘, 23(6): 186～201.
李锦轶. 2002. 湖北大洪山地区原"莲沱组"时代质疑. 地质通报, 21(8): 579～583.
李三忠, 张国伟, 李亚林, 赖绍聪,李宗会. 2002. 秦岭造山带勉略缝合带构造变形与造山过程. 地质学报, 76(4): 469～483.
李献华, 周国庆, 赵建新. 1994. 赣东北蛇绿岩的离子探针锆石 U-Pb 年龄及其构造意义. 地球化学, 23(2): 125～131.
凌文黎, 高山, 欧阳建平, 张本仁, 李惠民. 2002. 西乡群的时代与构造背景:同位素年代学及地球化学制约. 中国科学: 地球科学, 32(2): 101～112.
陆松年. 2001. 从罗迪尼亚到冈瓦纳超大陆——对新元古代超大陆研究几个问题的思考. 地学前缘, 8(4): 441～448.
陆松年, 相振群, 李怀坤, 王惠初, 初航. 2012. 华北克拉通对罗迪尼亚超大陆事件的响应——GOSEN 连接假设. 地质学报, 86(9): 1396～1406.
罗来, 贺良, 孙海清, 黄建中. 2016. 扬子东南缘高涧群底部锆石 SHRIMP U-Pb 年龄. 华南地质与矿产, 32(1): 15～20.
宋彪, 张玉海, 万渝生. 2002. 锆石 SHRIMP 样品靶制作、年龄测定及有关现象讨论. 地质论评, 48(增刊): 26～30.
宋芳, 牛志军, 何垚砚, 杨文强. 2016. 中扬子地区南华纪早期碎屑锆石 U-Pb 年龄及其对物源特征和古地理格局的约束. 地质学报, 90(10): 2661～2680.
王剑. 2000. 华南新元古代裂谷盆地演化——兼论与 Rodinia 解体的关系,北京:地质出版社, 1～146.
王涛, 张宗清, 王晓霞, 王彦斌,张成立. 2005. 秦岭造山带核部新元古代碰撞变形及其时代——强变形同碰撞花岗岩与弱变形脉体锆石 SHRIMP 年龄限定. 地质学报, 79(2): 220～231.
夏邦栋, 方中. 1989. 磨拉石与全球构造. 石油实验地质, 11(4): 314～319.
谢继锋, 张本仁. 2000. 秦岭勉略带中鞍子山蛇绿杂岩的地球化学——古洋壳碎片的证据及意义. 地质学报, 74(01): 39～50.
谢士稳, 高山, 柳小明, 高日胜. 2009. 扬子克拉通南华纪碎屑锆石 U-Pb 年龄、Hf 同位素对华南新元古代岩浆事件的指示. 地球科学, 34(1): 117～126.
徐大良, 刘浩, 魏运许, 彭练红, 邓新. 2016. 扬子北缘神农架地区郑家垭组碎屑锆石年代学及其构造意义. 地质学报, 90(10): 2648～2660.
许志琴, 李源, 梁凤华, 裴先治. 2015. "秦岭—大别—苏鲁"造山带中"古特提斯缝合带"的连接. 地质学报, 89(4): 671～680.
张恒, 高林志, 李廷栋, 耿树方, 刘燕学, 丁效忠, 史志刚. 2015. 浙西地区新元古代骆家门组 SHRIMP 锆石 U-Pb 年龄及其地质意义. 地质通报, 34(2-3): 447～455.
张雄, 曾佐勋, 潘黎黎, 曾智辉, 彭练红, 徐大良, 魏运许, 刘浩, 邓新. 2016. 对湖北大洪山地区一套紫红色砂—砾岩系沉积年代的再认识——碎屑锆石 U-Pb 年龄及其地质意义. 地质通报, 35(7): 1069～1080.
张忠英, 赵银胜. 1989. 湖北大洪山地区打鼓石群微体植物化石的发现. 地质论评, 35(1): 84～89.
张宗清, 张国伟, 唐索寒, 王进辉. 2001. 鱼洞子群变质岩年龄及秦岭造山带太古宙基底. 地质学报, 75(2): 198～204.

Depositional Age of the Huashan Group on the Northern Margin of the Yangtze Plate and Its Constraints on Breakup of the Rodinia Supercontinent

TIAN Hui[1), LI Huaikun[1), ZHOU Hongying[1), ZHANG Jian[1), ZHANG Kuo[1),
GENG Jianzhen[1), XIANG Zhenqun[1), QU Lesheng[2)

1) *Tianjin Center, China Geological Survey, Tianjin*, 300170;
2) *Hubei Institute of Regional Geology and Mineral Resources Survey, Wuhan*, 430034

Abstract

Outcropped in the Dahongshan area on the northern margin of the Yangtze Plate, the Huashan Group consists of a suite of coarse-grained clastic rocks dominated by conglomerates and a suite of fine-grained detrital sedimentary rocks characterized by sandy slate in an ascending order; with the deposition accompanied by tholiitic basaltic magmatism. The Huashan Group was formed in a complex tectonic background and underwent low-grade metamorphism. There have been long disputes about the tectonic attribute of the Huashan Group and the tempo-spatial relationship with the so-called Huanshan 'Ophiolite Complex'. However, they probably provide an important constraint on Rodinia supercontinent assembly-breakup events on the northern margin of Yangtze Plate. One sample of basaltic tuff interlayered in fine-grained sandstone in the lower Liufangzui Formation of the Huashan Group was collected for SHRIMP zircon U-Pb method dating, and three samples of clastic rocks (two from the Liufangzui Formation and one from the overlying Liantuo Formation of Nanhua System) were collected for LA-MC-ICPMS zircon U-Pb dating. We obtaind a zircon U-Pb age of 814.7 ± 7.3 Ma for the basaltic tuff. Detrital zircon U-Pb ages of clastic rocks of the Huashan Group have three peaks respectively at ~900 Ma, ~2050 Ma and ~2650 Ma, among which the most distinct one is ~2650 Ma. While the detrital zircon U-Pb ages of the clastic rock from the Liantuo Fotrmation also have three peaks at~900 Ma, ~2050 Ma and ~2500 Ma, with the most distinct peak at ~2050 Ma. The three samples of detrital zircons are similar to the clastic rocks of the Yangtze Plate in U-Pb age statistic peaks. The source for the clastic rocks of the Huashan Group might include the underlying Mesoproterozoic Dagushi Group, Archean Yudongzi Complex and Kongling Complex. Combined with the previous dating materials and regional tectonic research achievements, it can be concluded that the Huashan Group was probably formed in the time range of 820~815 Ma in an extensional environment, indicating that it is different from the Huashan "Ophiolite Complex" in terms of time and tectonic background. Huashan "Ophiolite Complex" and Huashan Group might reflect a tectonic regime transition from compression to extension respectively. Clastic sediments of the Huashan Group, along with mafic volcanic rocks and volcanoclastic rocks, are coeval sedimentary and volcanic formation formed in an extensional tectonic background. Based on previous discovery of a large volume of ~820 Ma felsic-mafic magmatic activity records and the contemporary strata (820~800 Ma) around the Yangtze Plate margins, it can be presumed that the Huashan Group deposited in the initial breakup stage of Rodinia supercontinent related to a super mantle plume.

Key words: Yangtze plate; Dahongshan; Huashan Group; Rodinia supercontinent